



**HAL**  
open science

# Do multi-sector energy system optimization models need hourly temporal resolution? A case study with an investment and dispatch model applied to France

Philippe Quirion, Behrang Shirizadeh

## ► To cite this version:

Philippe Quirion, Behrang Shirizadeh. Do multi-sector energy system optimization models need hourly temporal resolution? A case study with an investment and dispatch model applied to France. *Applied Energy*, 2022, 305, pp.117951. 10.1016/j.apenergy.2021.117951 . hal-03495892

**HAL Id: hal-03495892**

**<https://hal.science/hal-03495892>**

Submitted on 21 Dec 2021

**HAL** is a multi-disciplinary open access archive for the deposit and dissemination of scientific research documents, whether they are published or not. The documents may come from teaching and research institutions in France or abroad, or from public or private research centers.

L'archive ouverte pluridisciplinaire **HAL**, est destinée au dépôt et à la diffusion de documents scientifiques de niveau recherche, publiés ou non, émanant des établissements d'enseignement et de recherche français ou étrangers, des laboratoires publics ou privés.

# Do multi-sector energy system optimization models need hourly temporal resolution?

A case study with an investment and dispatch model applied to France

Behrang SHIRIZADEH<sup>1,2\*</sup>, Philippe QUIRION<sup>1</sup>

## Abstract

Energy system optimization models (ESOMs) increasingly cover the main energy-consuming sectors rather than just electricity, which massively raises calculation time. To reduce the latter, researchers apply various time-series aggregation methods, the pros and cons of which have been analyzed for electricity-only ESOMs but not for ESOMs also covering the main energy-consuming sectors. To address this question we compare the two main time-series aggregation methods: (1) reducing the temporal resolution (from one to two, four or eight hours) and (2) selecting representative periods (one week over one, two or three months, with an hourly resolution). We apply these methods to EOLES\_mv, an ESOM covering the main French energy sectors. Both methods cut the calculation time by a similar amount but the former generates much smaller discrepancies for the main output variables (energy mix, system cost and CO<sub>2</sub> emissions). These results are at odds with those generally obtained with electricity-only ESOMs, for which reducing the temporal resolution generates significant discrepancies when wind and solar dominate the electricity mix.

**Keywords:** Energy system modelling; Sector coupling; Time-series aggregation; Temporal resolution; Representative periods; Computational tractability.

---

<sup>1</sup> CIREN-CNRS, 45 bis avenue de La Belle Gabrielle, 94736 Nogent sur Marne Cedex, France

<sup>2</sup> Deloitte Economic Advisory, Tour Majunga, 6 Place de la Pyramide, 92908 Paris-la-Défense Cedex, France.

\*Corresponding author: shirizadeh@centre-cired.fr

# 1. Introduction

## 1.1. Motivation

To be of greatest use for climate and energy policies, energy system optimization models (ESOMs) should ideally include the main energy sectors, and optimally allocate the different energy sources and carriers to meet the end-use energy demand; this is referred to as ‘sector coupling’ (Brown et al., 2018a, Lund et al., 2017, Zhu et al., 2020).

Unfortunately, the optimization of an ESOM featuring sector coupling over a full year (let alone several years) with an hourly resolution at the country level (and even more for a whole continent) is computationally demanding. Not only does it require large amounts of memory, but the calculation time is very long. For example, with the ESOM we use in the present paper (Shirizadeh, 2021) optimization of a single scenario over one year requires more than 60 hours on a standard personal computer<sup>1</sup>. Therefore, finding ways to reduce the calculation time without sacrificing accuracy is particularly welcome for sector-coupled ESOMs, and avoiding the modeling of every hour in a full year would reduce the calculation time a lot. The question is to what extent this would reduce the accuracy of the results.

## 1.2. Previous studies

Most electricity-only ESOMs applied at the country scale and featuring a high proportion of wind and solar generation use hourly temporal resolution. This choice is justified by the literature: on the one hand, if the size of the modeled area is that of a large European State, hourly resolution suffices since for both wind and solar generation, sub-hourly fluctuations, which are significant at the local scale, cancel each other out (Brown et al., 2018b, and references therein). On the other hand, with a temporal resolution coarser than one hour, demand peaks and wind or solar generation troughs are smoothed, resulting in an underestimation of the generation and storage capacities necessary to satisfy electricity demand (Pfenninger, 2017, De Guibert et al., 2020).

An increasing number of ESOMs include coupling between electricity and the other energy sectors (mostly heat and transportation). As shown in the recent review by Prina et al. (2020), some of these sector-coupled ESOMs model a full year based on hourly resolution while others select representative periods (also called time slices), e.g. one week with an hourly resolution to represent a specific period that has similar hourly profile for all the weeks in the studied period. Hoffmann et al. (2020) review the development of both time-series aggregation methods (temporal resolution reduction and representative period selection) and their implementation in ESOMs.

---

<sup>1</sup> The computer has 128 GB of RAM and its CPU is an Intel® Xeon® Bronze 3106 with 8 cores at 1.7 GHz.

### 1.3. Research gaps

While representative period selection is widely applied, e.g. in the TIMES models<sup>1</sup>, only a few studies mentioned in the exhaustive survey by Hoffmann et al. (2020) apply resolution reduction, and to our knowledge, none of them apply the latter method to sector-coupled ESOMs.

Although the need for hourly temporal resolution has been established for electricity-only country-size ESOMs (Brown et al., 2018b), this result does not necessarily hold for sector-coupled ESOMs. Indeed, sector coupling might mitigate the impact of demand peaks and wind or solar generation troughs, thanks to flexibility gains from non-electricity energy sectors (Victoria et al., 2019; Gea-Bermúdez et al., 2021). Therefore, the required temporal resolution might be coarser than one hour, unlike for electricity-only ESOMs.

### 1.4. Study aims

Our broad research question is the following: what time-series aggregation method works best (in terms of results accuracy and calculation time) for a multi-sector ESOM featuring sector-coupling? To the best of our knowledge, this is the first paper to address this question for a multi-sector ESOM.

We apply the two above-mentioned time-series aggregation methods (temporal resolution reduction and representative period selection) to a multi-sector capacity expansion ESOM applied to France: EOLES\_mv (which stands for Energy Optimization for Low Emission Systems - multi-vector; Shirizadeh, 2021). To this end, we develop seven different versions of the EOLES\_mv model. Four represent a full year with constant temporal resolution (time steps of one, two, four and eight hours), while three use representative periods, in this case weeks (one per month, one per two months and one per three months) for a full year.

We conclude that temporal resolution reduction provides a much better trade-off between the calculation time and the output discrepancies than selection of representative periods. Moreover, the former method generates very small discrepancies even if the temporal resolution is as coarse as eight hours, while the calculation time is reduced 640-fold. This result still holds when we exclude nuclear energy, which results in an optimal energy mix of which 98% comes from renewable energy sources.

As a final check, we optimize investment at coarse temporal resolution (two, four or eight hours) and then optimize dispatch with an hourly resolution, to analyze whether the resulting lost electricity load changes the results. Discrepancies remain very small, which further confirms our main result.

---

<sup>1</sup> The TIMES (The Integrated MARKAL-EFOM System) models, initially developed by the International Energy Agency, are widely used energy system optimization models. They are based on sequential optimization: first investment and later operation (dispatch) of the energy system. These models represent either one energy sector (electricity in Krakowski et al., 2016), or several sectors (electricity and gas in Doudard, 2018), they represent either one country (the previously cited versions) or a larger area (for example the world in Kang, 2017). They all rely on representative period selection, such as one week-day and one weekend-day per month (Doudard, 2018) or different number of time-slices per year (for example 84 time-slices in Krakowski et al., 2016).

The remainder of this paper is organized as follows. Sections 2 and 3 present the methods (the different versions of the EOLES\_mv model) and the input data, Section 4 presents the results and Section 5 concludes.

## 2. Methods

### 2.1. The EOLES\_mv model

We use EOLES\_mv, which belongs to the EOLES (Energy Optimization for Low Emission Systems) family of models. The EOLES family of models performs simultaneous optimization of the investment in and the operation of the energy system in order to minimize the total cost while satisfying energy demand *on an hourly basis*. The electricity-only versions of the EOLES family of models (Shirizadeh et al., 2022; Shirizadeh and Quirion, 2021) are representative of other capacity expansion models like DIETER (Schill and Zerrahn, 2018), FLORE (Perrier, 2018) or Calliope (Pfenninger, 2017).

The “mv” in EOLES\_mv stands for multi-vector and this model minimizes the annualized energy generation, conversion and storage costs, including the cost of connection to the grid. EOLES\_mv considers all the major energy sectors (residential and tertiary buildings, industry, transport and agriculture) in an integrated manner, enabling sector-coupling. It is similar to other recent multi-sector capacity expansion models such as those presented in Brown et al. (2018a), Gea-Bermúdez et al. (2021), Henning and Palzer (2014), Prina et al. (2020), Victoria et al. (2019), as well as Zhu et al. (2019). However, not all these models cover every sector included in EOLES\_mv, and the geographical coverage differs across these models.

EOLES\_mv is a greenfield optimization model, which calculates a cost-optimal steady state, taking into account the main technical and resource availability constraints. Therefore, this model does not produce a dynamic trajectory but a static optimal state. In order to account for precise dispatch with correct dimensioning of storage technologies and the seasonal and intra-daily variability of demand and energy production from renewable resources, the selected optimization period is a full year with hourly time-steps.

As all the optimization of dispatch and investment models, EOLES\_mv is used for the capacity expansion of the considered system. This model shows the lowest cost future energy system, based on the hypotheses in the considered time horizon. Optimization of investment is the enabler of this functionality of the model. However, to make sure both the short-term and long-term (seasonality) variability of renewable sources and energy demand are correctly taken into account, hourly energy production and storage operation profiles are optimized. The latter is the optimization of the dispatch. Therefore, thanks to simultaneous optimization of both, a functioning optimal future energy system is the result of this model which can be used to (1) introduce a national optimal low-carbon future energy system target, (2) study the impact of different policy measures in the evolution of the energy system, (3) provide investment advisory based on the future technologies and (4) simulate the hourly operation of power system and identify the main economic characteristics of the future energy market.

This model considers a country as a single node using the copper-plate assumption: spatial optimization is, therefore, not considered in this model. Although including spatial optimization and therefore transmission costs can increase or decrease the overall system cost, in a previous article we showed that modeling France as a single node while assuming that onshore wind and solar capacities are located in proportion to existing facilities (which is the case in this study) leads to

much faster calculation (240 times) than considering France as four nodes, with negligible error in installed capacity of the key technologies and the overall cost of the system (Shirizadeh et al., 2022).

The EOLES\_mv model includes seven power generation technologies: floating and monopile offshore wind power, onshore wind power, photovoltaic solar power (PV), run-of-river and lake-generated hydro-electricity, nuclear power (EPR, i.e. third generation European Pressurized Water Reactors) and three gas production technologies: natural (fossil) gas, methanization from anaerobic digestion and pyro-gasification of solid biomass. Sector-coupling is enabled by vector-change (energy conversion) technologies: open-cycle gas turbines (OCGT), combined-cycle gas turbines (CCGT) and CCGTs equipped with post-combustion carbon capture and storage (CCS) technologies are used to convert gas to electricity. Vector-change from electricity to gas is enabled by electrolysis (power to hydrogen to inject into the gas network with a volume share limit) and methanation (hydrogen production from electrolysis of water and use of the Sabatier reaction between the hydrogen thus produced and green CO<sub>2</sub> to produce synthetic methane) as power-to-gas options. Similarly, centralized and decentralized boilers are used to produce heat from gas while centralized and individual heat pumps and resistive heat production technologies are used to produce heat from electricity. The model includes two electricity storage technologies (Li-Ion batteries and pumped hydro storage), the existing gas network as the gas storage option and two heat storage technologies (centralized and decentralized hot water tanks). Moreover, EOLES\_mv allows demand for transport to be met with an endogenous choice between electric vehicles and internal combustion engine vehicles, for three main transport categories: light vehicles, heavy vehicles and buses (trains are all set to be electric since they are currently electric in France). The interactions of different energy end-use demands, supply side, storage and energy carriers are presented in Figure 1.

The EOLES\_mv model is based on representative technologies chosen from groups of technologies with similar technical and economic behavior. For instance, only two engine types are considered in the transport sector: gas-fueled internal combustion engine (ICE) vehicles and battery electric vehicles (BEV). Other transport options include liquid-fueled ICE vehicles and hydrogen-fueled fuel cell electric vehicles but since they have similar economic and technical behavior to gas-fueled ICE vehicles and BEVs respectively, they have been excluded in order to maintain computational tractability.

The main simplification assumptions in the EOLES family of models are as follows: demand is inelastic, and the optimization is based on full information about the weather and electricity demand. This model uses only linear optimization: non-linear constraints might improve accuracy, especially when studying unit commitment, but they entail significant increase in computation time. Palmintier (2014) has shown that linear programming provides an interesting trade-off, with little impact on cost, CO<sub>2</sub> emissions and investment estimations, but speeds up processing by up to 1,500 times. The model is written in GAMS and solved using the CPLEX solver. In the current study, we provide a greenfield optimization by considering continental France as an isolated country for the year 2050.

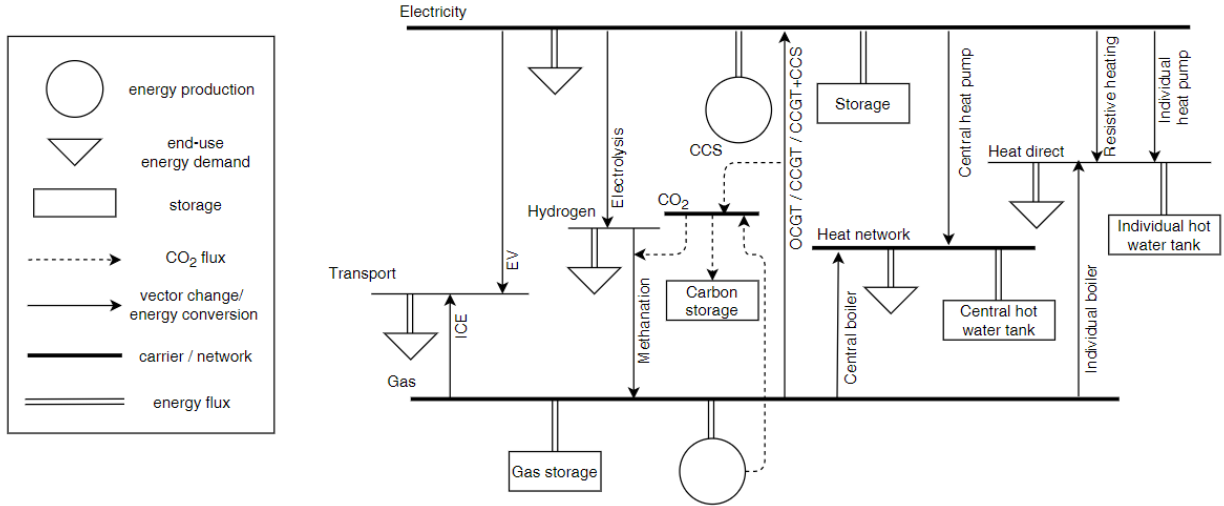


Figure 1. Interactions between energy supply, demand, storage and carriers by energy flux and CO<sub>2</sub> exchanges in the EOLES\_mv model. The horizontal lines show the different final energy forms, as well as the CO<sub>2</sub> network. Among these horizontal lines, the bold ones are energy carriers (except CO<sub>2</sub> which is a feedstock). The interactions between the different energy carriers and end-uses are enabled by vertical arrows that represent vector-change technologies: power-to-gas, gas-to-power, power-to-heat, gas-to-heat, power-to-transport and gas-to-transport. Transport is modelled as a demand that has the form of distance travelled. The circles represent the energy supply technologies that are connected to their primary energy forms, and they satisfy different end-uses represented as triangles. To distinguish between energy and feedstock flow, we represent the CO<sub>2</sub> flux in dashed lines. All the above-mentioned interactions are modelled by the constraint equations of the EOLES\_mv model.

A more detailed description of the EOLES\_mv model can be found in Shirizadeh (2021). The sets, parameters, variables and equations of the model with hourly resolution can be found in Appendix 1. All the versions of the EOLES\_mv model and their input data are available on GitHub<sup>1</sup>.

## 2.2. Resolution variation

To account for the importance of temporal resolution, we developed several versions of the model using two-, four- and eight-hour resolutions. These coarser-resolution versions reduce the number of time-steps from 8760 to 4380, 2190 and 1095 respectively. To adapt the EOLES\_mv model to each of these time-steps, the original equations (Equations (A.1), (A.12), (A.16), (A.19), (A.20), (A.21), (A.25), (A.27), (A.29), (A.32) and (A.34) presented in Appendix 1) have been modified respectively (Equations 1 to 11 in Box 1).

Equation (I) (A.1 in Appendix 1) is the objective function to be minimized, which is the social cost function.

$$\begin{aligned}
 COST = & \left( \sum_{tec} [(Q_{tec} - q_{tec}^{ex}) \times annuity_{tec}] + \sum_{str} (VOLUME_{str} \times annuity_{str}^{en}) \right. \\
 & \left. + \sum_{tec} (Q_{tec} \times fO\&M_{tec}) + \sum_{tec} \sum_h (G_{tec,h} \times (vO\&M_{tec} + e_{tec} SCC_{CO_2})) \right) / 1000
 \end{aligned}
 \tag{I}$$

Where  $Q_{tec}$  represents the production capacities,  $q_{tec}^{ex}$  represents the existing capacity (notably for hydro-electricity technologies with long lifetime),  $VOLUME_{str}$  is the energy storage capacity in

<sup>1</sup> [https://github.com/BehrangShirizadeh/EOLES\\_mv\\_temp](https://github.com/BehrangShirizadeh/EOLES_mv_temp)

GWh,  $S_{str}$  is the storage capacity in GW, *annuity* is the annualized investment cost, *fO&M* and *vO&M* respectively represents fixed and variable operation and maintenance costs,  $G_{tec,h}$  is the hourly generation of each technology,  $e_{tec}$  is the specific emission of each technology in tCO<sub>2</sub>/GWh of power production and  $SCC_{CO_2}$  is the social cost of carbon in €/tCO<sub>2</sub>.

This equation represents the sum of all costs over the chosen period, including the annualized investment costs as well as the fixed and variable O&M costs, and the penalty associated to CO<sub>2</sub> emissions, i.e. the ‘Social Cost of Carbon’ (SCC)<sup>1</sup>. For some storage options, another CAPEX-related cost proportional to the energy capacity in €/kWh is accounted for (*annuity<sub>str</sub><sup>en</sup>*). It is modified to Equation (1) in Box 1 by inclusion of the parameter  $l_{res}^{ts}$  which is the correction factor to account for the full energy production over a year by each technology.

In Equation (II) (A.12 in Appendix 1), monthly available energy for the hydroelectricity generated by lakes and reservoirs is defined using monthly lake inflows which means that energy stored can be used within the month but not across months.

$$lake_m \geq \sum_{h \in m} G_{lake,h} \quad (II)$$

Where  $G_{lake,h}$  is the hourly power production by lakes and reservoirs, and  $lake_m$  is the maximum electricity that can be produced from this energy resource in one month. Equation (2) adapts it to different time-steps using the length of the considered time-step (parameter  $l_{res}^{ts}$ ).

Equation (III) (A.16 in Appendix 1) defines the reservoir size of the mobility technologies.

$$\sum_{h \in w} CHARGE_{transport,h} \leq RESERVOIR_{transport} \quad (III)$$

Where  $RESERVOIR_{transport}$  accounts for the reservoir size of each transport technology (kWh<sub>e</sub> for electric vehicles and kWh<sub>th</sub> for ICE vehicles). The storage volume of each transport technology accounts for an upper limit for the weekly charge and weekly energy consumption of it. While this storage volume is free of charge for ICE vehicles, electric vehicles’ main cost component is this battery storage volume. Its adaptation to coarser-than-hourly time-steps leads to Equation (3).

For open-cycle and combined-cycle gas turbines, there are some safety- and maintenance-related breaks. Equations (IV), (V) and (VI) (A.19, A.20 and A.21 in Appendix 1) limit the annual power production for each of these plants to their maximum annual capacity factors, and Equations (4), (5) and (6) in Box 1 are the modified versions for the resolution variation cases by the inclusion of the length of time-step parameter ( $l_{res}^{ts}$ ).

$$\sum_h G_{ocgt,h} \leq Q_{ocgt} \times cf_{ocgt} \times 8760 \quad (IV)$$

$$\sum_h G_{ccgt,h} \leq Q_{ccgt} \times cf_{ccgt} \times 8760 \quad (V)$$

$$\sum_h G_{ccgt-ccs,h} \leq Q_{ccgt-ccs} \times cf_{ccgt-ccs} \times 8760 \quad (VI)$$

Where  $cf_{ocgt}$  and  $cf_{ccgt}$  are the capacity factors of OCGT and CCGT power plants.

Nuclear power plants have limited flexibility, so definitions of hourly ramp-up and ramp-down rates matter to model them accurately. Equations (VII) and (VIII) (A.25 and A.26 in Appendix 1) limit the power production of nuclear power plants with these ramping constraints.

$$G_{nuc,h+1} + RSV_{nuc,h+1} \leq G_{nuc,h} + r_{nuc}^{up} \times Q_{nuc} \quad (VII)$$

<sup>1</sup> For the value of the SCC parameter, we have chosen the one which allows carbon neutrality (an official target of France for 2050) in the EOLES\_mv model, i.e. €200/tCO<sub>2</sub>.



$$G_{nuc,h+1} \geq G_{nuc,h}(1 - r_{nuc}^{down}) \quad (VIII)$$

Where  $G_{nuc,h+1}$  is the nuclear power production at hour  $h + 1$ ,  $G_{nuc,h}$  is the nuclear power production at hour  $h$ ,  $RSV_{nuc,h+1}$  is the reserve capacity provided by nuclear power plants at hour  $h + 1$  and  $r_{nuc}^{up}$  and  $r_{nuc}^{down}$  are the ramp-up and ramp-down rates for nuclear power production.

Only Equation (VII) is translated for the coarse temporal resolutions, since the nuclear ramp rate is 50% and for coarser temporal resolutions (2-, 4- and 8-hour) this limit does not apply. Moreover, the nuclear power plants' capacity factor should also be limited by safety and maintenance constraints (Equation IX, A.27 in Appendix 1).

$$\sum_h G_{nuc,h} \leq Q_{nuc} \times cf_{nuc} \times 8760 \quad (IX)$$

Where  $cf_{nuc}$  is the maximum annual capacity factor of nuclear power plants. Equations (VII) and (IX) are translated to Equations (7) and (8) in Box 1.

Equations (X) to (XII) (A.8, A.28 and A.29 in Appendix 1) define the storage mechanism and constraint in terms of power. The two first equations don't need to be adapted to varying temporal resolution cases. Indeed, since the parameters are defined by taking an average over the hours in the considered time-step, the resulting hourly variables (STORAGE and G) are hourly values, as if they were repeated consequently at each hour during the whole time-step as the same value.

However, the equation that limits the available volume of energy that can be stored by each storage option (Equation XII) should be modified to take into account the length of the time-steps (Equation 9 in Box 1).

$$SOC_{str,h+1} = SOC_{str,h} + (STORAGE_{str,h} \times \eta_{str}^{in}) - \left(\frac{G_{str,h}}{\eta_{str}^{out}}\right) \quad (X)$$

$$SOC_{str,0} = SOC_{str,8759} + (STORAGE_{str,8759} \times \eta_{str}^{in}) - \left(\frac{G_{str,8759}}{\eta_{str}^{out}}\right) \quad (XI)$$

$$SOC_{str,h} \leq VOLUME_{str} \quad (XII)$$

Where  $SOC_{str,h}$  is the state of charge of the storage option  $str$  at hour  $h$ , while  $\eta_{str}^{in} \in [0,1]$  and  $\eta_{str}^{out} \in [0,1]$  are the charging and discharging efficiencies.  $STORAGE_{str,h}$  is the discharge of the storage technology  $str$  at hour  $h$ .

The captured carbon dioxide can't be stored infinitely, and geographical and social constraints limit the exploitation of CCS technology. Equation (XIII) (A.34 in Appendix 1) introduces this limit, which is translated to Equation (10).

$$\varphi_{CO_2}^{max} \geq \sum_h G_{ccgt-ccs,h} \times \tau_{ccgt-ccs} \times e_{ccgt} \quad (XIII)$$

Where  $\varphi_{CO_2}^{max}$  is the maximal CO<sub>2</sub> storage potential,  $G_{ccgt-ccs,h}$  is hourly power production from CCGT power plants equipped with CCS units,  $\tau_{ccgt-ccs}$  is the carbon capture rate of post combustion CCS units, and  $e_{ccgt}$  is the specific emission of CCGT power plant with natural gas (considered with no CCS input).

Equation (XIV) (A.32 in Appendix 1) limits the annual renewable gas production from each of two renewable gas production technologies; methanization and pyro-gasification of biomass, and its modified version is in Equation (11) in Box 1.

$$\sum_{h=0}^{8759} G_{biogas,h} \leq g_{biogas}^{max} \quad (XIV)$$

Where  $G_{biogas,h}$  is the hourly biogas production from each of renewable gas production technologies and  $g_{biogas}^{max}$  is the maximal yearly biogas that can be produced from each of renewable gas production technologies, both in energy values.

Using the time-step length parameter ( $l_{res}^{ts}$ ) all the above-mentioned equations are translated into the equations in Box 1.

Box 1. The modified equations of EOLES\_mv model to adapt it to coarser-than-hourly temporal resolutions

$$COST = [\sum_{tec}((Q_{tec} - q_{tec}^{ex}) \times annuity_{tec}) + \sum_{str}(VOLUME_{str} \times annuity_{str}^{en}) + \sum_{tec}(Q_{tec} \times fO\&M_{tec}) + \sum_{tec} \sum_{ts}(G_{tec,ts} \times l_{res}^{ts} \times (vO\&M_{tec} + e_{tec} \times SCC_{CO_2}))]/1000 \quad (1)$$

$$lake_m \geq \sum_{ts \in m} G_{lake,ts} \times l_{res}^{ts} \quad (2)$$

$$\sum_{ts \in w} CHARGE_{transport,ts} \times l_{res}^{ts} \leq RESERVOIR_{transport} \quad (3)$$

$$\sum_{ts} G_{ocgt,ts} \times l_{res}^{ts} \leq Q_{ocgt} \times cf_{ocgt} \times 8760 \quad (4)$$

$$\sum_{ts} G_{ccgt,ts} \times l_{res}^{ts} \leq Q_{ccgt} \times cf_{ccgt} \times 8760 \quad (5)$$

$$\sum_{ts} G_{ccgt-ccs,ts} \times l_{res}^{ts} \leq Q_{ccgt-ccs} \times cf_{ccgt-ccs} \times 8760 \quad (6)$$

$$G_{nuc,ts+1} + RSV_{nuc,ts+1} \leq G_{nuc,ts} + r_{nuc}^{up} \times Q_{nuc} \times l_{res}^{ts} \quad (7)$$

$$\sum_{ts} G_{nuc,ts} \times l_{res}^{ts} \leq Q_{nuc} \times cf_{nuc} \times 8760 \quad (8)$$

$$SOC_{str,ts} \times l_{res}^{ts} \leq VOLUME_{str} \quad (9)$$

$$\varphi_{CO_2}^{max} \geq \sum_h G_{ccgt-ccs,h} \times \tau_{ccgt-ccs} \times e_{ccgt} \times l_{res}^{ts} \quad (10)$$

$$\sum_{ts} G_{biogas,ts} \times l_{res}^{ts} \leq g_{biogas}^{max} \quad (11)$$

### 2.3. Representative periods

Representative periods can take several forms to account for different variations. Doudard (2018) considers 576 time-slices per year, by considering one weekday and one weekend day for each month. Samsatli et al. (2016) use one weekday and one weekend day for each season, resulting in 192 time-slices for each year. Although weekday and weekend classification accounts for the difference between a working day and weekend, it does not capture differences between weekdays or between the two days of the weekend. To overcome this issue, Perrier (2018) chooses a representative week over a two-month period. In this paper, we follow the same method, by choosing a representative week taking the average of all the weeks in one month, two months and

three months. Thus, each day of the week is repeated identically each time it appears in the month. Considering one representative week per month, one representative week per two months and one representative week per three months reduces the number of time-slices from 8760 to 2016, 1008 and 672 respectively.

To adapt the EOLES\_mv model to this time-series aggregation method, we defined two different storage types: short- & medium-term storage options which can be fully charged and discharged in one week, and long-term storage options which can be fully charged and discharged in one month, two months or three months. In a continuous period, the storage options operate endogenously depending on their economic characteristics and technical limits: a storage option with high energy capacity cost and low power capacity cost, such as batteries, will operate as a short-term storage option, while a technology with low energy capacity cost and high power capacity cost, such as methanation storage, will operate as a long-term storage option (Shirzadeh et al., 2022 and Schill and Zerrahn 2018).

However, in a model with non-continuous periods, the charging and discharging cycles must be defined exogenously because from a modelling perspective it is necessary to know whether the operation of a storage technology will be repeated during each week of the chosen period to be represented or if it will be added up during the whole chosen period to be represented. For instance, the state of charge of a short-term storage option at the end of one representative week should equal the state of charge of that storage option at the beginning of the next representative week (cyclicality constraint), but the state of charge of a long-term storage option at the beginning of a representative week is its state of charge at the end of the previous representative week multiplied by the number of weeks in the considered period to be represented by a week. To apply this condition, Equation (X) (A.8 in Appendix 1) which was introduced in subsection is modified and divided into three equations (Equations 12, 13 and 14 in Box 2).

Box 2. Definition of long-term and short-term storage options in EOLES\_mv models with representative periods

$$SOC_{str\_short,h+1} = SOC_{str\_short,h} + (STORAGE_{str\_short,h} \times \eta_{str\_short}^{in}) - \left(\frac{G_{str\_short,h}}{\eta_{str\_short}^{out}}\right) \quad (12)$$

$$\forall \begin{cases} h \in w \\ h+1 \in w \end{cases};$$

$$SOC_{str\_long,h+1} = SOC_{str\_long,h} + (STORAGE_{str\_long,h} \times \eta_{str\_long}^{in}) - \left(\frac{G_{str\_long,h}}{\eta_{str\_long}^{out}}\right) \quad (13)$$

$$\forall \begin{cases} h \in w \\ h+1 \notin w \end{cases};$$

$$SOC_{str\_long,h+1} = SOC_{str\_long,h} \times l_w^p + (STORAGE_{str\_long,h} \times \eta_{str\_long}^{in}) - \left(\frac{G_{str\_long,h}}{\eta_{str\_long}^{out}}\right) \quad (14)$$

Energy entering storage option  $str$  at hour  $h$ ,  $G_{str\_long,h}$  is the energy generation (discharging) of storage option  $str$  at hour  $h$ , while  $\eta_{str}^{in} \in [0,1]$  and  $\eta_{str}^{out} \in [0,1]$  are the charging and discharging efficiencies.  $str\_short$  represents short-term storage technologies (Li-Ion batteries, PHS and individual thermal energy storage),  $str\_long$  represents long-term energy storage options (gas storage and central thermal energy storage).  $w$  represents the week and  $l_w^p$  is the relative length of the chosen period to the representing week, which is equal to the number of hours in the chosen period divided by the number of hours in a week (168).

Equations (I), (II), (IV), (V), (VI), (IX), (XII), (XIII) and (XIV) in the previous section have been modified respectively as in that section. Box 2 summarized these equations.

In Box 3,  $l_{ratio}^p$  is the ratio of the real length of a whole year to the represented fraction of the year which is equal to 8760/2016 for one week representing one month, 8760/1008 for one week representing two months and 8760/672 for one week representing three months.

Box 3. The modified equations of EOLES\_mv to adapt them to the models with representative periods

$$COST = (\sum_{tec} [(Q_{tec} - q_{tec}^{ex}) \times annuity_{tec}] + \sum_{str} (VOLUME_{str} \times annuity_{str}^{en}) + \sum_{tec} (Q_{tec} \times fO\&M_{tec}) + \sum_{tec} \sum_h (G_{tec,h} \times l_{ratio}^p \times (vO\&M_{tec} + e_{tec} SCC_{CO_2}))) / 1000 \quad (15)$$

$$lake_m \geq \sum_{h \in m} G_{lake,h} \times l_w^p \quad (16)$$

$$\sum_w \sum_{h \in w} G_{ocgt,h} \times l_w^p \leq Q_{ocgt} \times cf_{ocgt} \times 8760 \quad (17)$$

$$\sum_w \sum_{h \in w} G_{ccgt,h} \times l_w^p \leq Q_{ccgt} \times cf_{ccgt} \times 8760 \quad (18)$$

$$\sum_w \sum_{h \in w} G_{ccgt-ccs,h} \times l_w^p \leq Q_{ccgt-ccs} \times cf_{ccgt-ccs} \times 8760 \quad (19)$$

$$\forall \left\{ \begin{array}{l} h \in w \\ h+1 \in w \end{array} \right\}; G_{nuc,h+1} + RSV_{nuc,h+1} \leq G_{nuc,h} + r_{nuc}^{up} \times Q_{nuc} \quad (20)$$

$$\forall \left\{ \begin{array}{l} h \in w \\ h+1 \in w \end{array} \right\}; G_{nuc,h+1} \geq G_{nuc,h} (1 - r_{nuc}^{down}) \quad (21)$$

$$\sum_w \sum_{h \in w} G_{nuc,h} \times l_w^p \leq Q_{nuc} \times cf_{nuc} \times 8760 \quad (22)$$

$$\varphi_{CO_2}^{max} \geq \sum_w \sum_{h \in w} G_{ccgt-ccs,h} \times \tau_{ccgt-ccs} \times e_{ccgt} \times l_w^p \quad (23)$$

$$\sum_w \sum_{h \in w} G_{biogas,h} \times l_w^p \leq g_{biogas}^{max} \quad (24)$$

### 3. Input data

In this section we present the input data briefly. The time horizon considered is 2050, which is also the official target date of the French government in reaching carbon neutrality. A more detailed description of the preparation of hourly profiles can be found in Shirizadeh (2021).

#### 3.1. VRE profiles

The hourly variable renewable load factors are taken from the ‘renewables.ninja’<sup>1</sup> website (Pfenninger and Staffel, 2016 and Staffel and Pfenninger, 2016). We choose one point per each county of France (*département*), and, assuming that onshore wind and solar capacities remain proportional to the existing ones, we aggregate the hourly load factors of the 95 counties to one single node. For solar power, we specify 10% of system loss, and for onshore wind power, we chose Vestas V90 2000 wind turbine with a hub height of 80 meters.

<sup>1</sup> <https://www.renewables.ninja/>

Offshore wind power profiles are based on the existing projects taken from '4C offshore'<sup>1</sup> website, but we eliminate the projects from the Mediterranean Sea. All the floating offshore projects are considered floating, and all the mounted projects are considered to be on monopile foundation. The wind turbine assumed for offshore wind power is Siemens SWT 4.0 130 with a hub height of 120 meters.

In a previous work, we showed that 2006 can be chosen as the representative year for the period of 2000-2018 regarding the weather variability of VRE technologies; thus, we use the hourly VRE and hydro-electricity profiles for the year 2006 (Shirizadeh et al., 2022).

### 3.2. Energy demand

The energy demand is categorized for each end-use: electricity, heat, transport and hydrogen (as a substitute for coal in the industry) covering all the main energy sectors: residential and tertiary buildings, industry and construction, agriculture and transport sectors. The preparation of energy demand profiles is explained in detail in Shirizadeh (2021), Table 1 shows the annual energy demand values, their hourly profiles and their sources.

Table 1. Sectorial demands for each end-use

Sector	End-use	Annual Value (Mtoe)	source	Profiles from	
Residential	Electricity	6.2	ADEME (2017), DGEC (2019)	ADEME (2015)	
	Heat	18.5		Doudard (2018)	
Tertiary	Electricity	7.2	ADEME (2017), DGEC (2019)	ADEME (2015)	
	Heat	7.1		Doudard (2018)	
Agriculture	Electricity	1.4	ADEME (2017), négaWatt (2017)	ADEME (2015)	
	Heat	1.6			
Industry	Electricity	6.7	ADEME (2017), négaWatt (2017)	ADEME (2015)	
	Heat	12.7		Flat <sup>2</sup>	
	Hydrogen	3.5	ADEME (2017)	Flat	
Transport	Passengers (in Gp.km)	Light	554	ADEME (2017)	Doudard (2018)
		public	51		
		Train	187		Flat
	Freight (in Gt.km)	Heavy	347		Doudard (2018)
		Train	127		Flat

### 3.3. Economic parameters

#### 3.3.1. Features of the technologies modeled

Tables 2, 3 and 4 show the economic parameters of energy production, conversion and storage technologies, and their sources.

<sup>1</sup> <https://www.4coffshore.com/>

<sup>2</sup> Flat profile means a profile that has the same value for all the time-steps. Thus, once the values are plotted as a function of the time-steps, the graph shows a flat horizontal line.

Table 2. Economic parameters of energy supply technologies

Technology	Overnight costs (€/kW)	Lifetime (years)	Annuity (€/kW/year)	Fixed O&M (€/kW/year)	Variable O&M (€/MWh)	Construction time (years)	Source
Offshore wind farm - floating	3,660	30	236.2	73.2	0	1	JRC (2017)
Offshore wind farm - monopile*	2,330	30	150.9	47	0	1	JRC (2017)
Onshore wind farm*	1,130	25	81.2	34.5	0	1	JRC (2017)
Solar PV*	423	25	30.7	9.2	0	0.5	JRC (2017)
Hydroelectricity – lake and reservoir	2,275	60	115.2	11.4	0	1	JRC (2017)
Hydroelectricity – run-of-river	2,970	60	150.4	14.9	0	1	JRC (2017)
Nuclear power	3,750	60	262.6	97.5	9.5**	10	JRC (2014)
Natural (fossil) gas	-	-	-	-	23.5***	-	IEA (2019)
Methanization	370****	20	29.7	37	50	1	ADEME (2018)
Pyro-gasification	2500	20	200.8	225	32*****	1	ADEME (2018)

\*For offshore wind power on monopiles at 30km to 60km from the shore, for onshore wind power, turbines with medium specific capacity (0.3kW/m<sup>2</sup>) and medium hub height (100m) and for solar power, an average of the costs of utility scale, commercial scale and residential scale systems without tracking are taken into account. In this cost allocation, we consider solar power as a simple average of ground-mounted, rooftop residential and rooftop commercial technologies. For lake and reservoir hydro we take the mean value of low-cost and high-cost power plants.

\*\*This variable cost accounts for €2.5/MWh-e of fuel cost and €7/MWh of other variable costs, excluding waste management and insurance costs.

\*\*\* The price projected for Europe in 2040 in the sustainable development scenario, standing for \$7.5/MBtu.

\*\*\*\*The overnight cost for methanization is the investment cost of the purification plants for syngas.

\*\*\*\*\*The overnight cost only accounts for the gasification plants, while the wood used for energy is accounted for in variable costs.

Table 3. Economic parameters of energy conversion technologies

Technology	Overnight costs (€/kW)	Lifetime (years)	Annuity (€/kW/year)	Fixed O&M (€/kW/year)	Variable O&M (€/MWh)	Construction time (years)	Conversion efficiency	Source
OCGT	550	30	35.28	16.5	0	1	0.45	JRC (2014)
CCGT	850	30	54.53	21.25	0	1	0.63	JRC (2014)
CCGT-CCS	1280	30	82.12	32	5.76*	1	0.55	JRC (2017)
Electrolysis (Power-to-H <sub>2</sub> )	450	25	31.03	6.75	0	0.5	0.8	ENEA (2016)
Methanation (Power-to-CH <sub>4</sub> )**	450/700	25/20	86.05	59.25	5***	0.5	0.8/0.79	ENEA (2016)
Resistive	100	20	7.86	2	0	0.5	0.9	Brown et al. (2018b)
Individual heat pump	1050	20	82.54	36.75	0	0.5	3.5	Henning and Palzer (2014)
Central heat pump	700	20	55.02	24.5	0	0.5	2	Henning and Palzer (2014)
Central gas boiler	63	20	4.95	0.945	0	0.5	0.9	Brown et al. (2018b)
Decentral gas boiler	175	20	13.76	3.5	0	0.5	0.9	Brown et al. (2018b)

\* This variable cost accounts for a 500km CO<sub>2</sub> transport pipeline and offshore storage costs estimated by Rubin et al. (2015).

\*\*Methanation is the combination of hydrogen production from electrolysis and the Sabatier reaction of green CO<sub>2</sub> as a by-product from methanization with the hydrogen produced, therefore the economic parameters of each production are presented as

electrolysis/Sabatier.

\*\*\*As in Shirizadeh et al. (2020).

Table 4. Economic parameters of energy storage technologies

Technology	Overnight costs (€/kW)	CAPEX (€/kWh)	Lifetime (years)	Annuity (€/kW/year)	Fixed O&M (€/kW/year)	Variable O&M (€/MWh)	Storage annuity (€/kWh/year)	Construction time (years)	Efficiency (input / output)	Source
Pumped hydro storage (PHS)	500	5	55	25.8050	7.5	0	0.2469	1	95%/90%	FCH-JU (2015)
Battery storage (Li-Ion)	140	100	12.5	15.2225	1.96	0	10.6340	0.5	90%/95%	Schmidt (2019)
ITES	0	18.38	20	-	0	0	1.4127	0.5	90%/90%	Brown et al. (2018b)
CTES	0	0.64	40	-	0	0	0.0348	1	90%/75%	Brown et al. (2018b)
Gas storage*	0	0	80	0	0	2	0	-	100%/99%	CRE (2018)

\*The French gas network is already operational for methane injection; therefore, no network development cost is considered. However, the network usage fee of €2/MWh<sub>th</sub> for the gas network is derived from the French energy regulation commission (CRE, 2018).

Table 5 shows the economic parameters for the two types of vehicle engine technologies considered, internal combustion engines fuelled with compressed gas and electric vehicles.

Table 5. Economic parameters of two vehicles engine types: internal combustion engines fuelled with compressed gas and battery electric vehicles (including their charging infrastructure)

Technology	Charging infrastructure (€/kW)	Reservoir (€/kWh)	Lifetime (years)	Charging annuity (€/kW/year)	Reservoir annuity (€/kWh/year)	Source
Electric vehicles	81.7*	100	10	11.08	12.64	CGDD (2017)
ICE vehicles	180**	0	15	17.14	0	Doudard (2018)

\*We consider a charging point cost of €600 for 7kW of charging power.

\*\*According to Doudard (2018), a gas charging station which can serve 400 vehicles per day costs €300,000: assuming nearly 100kWh<sub>th</sub> (384km of autonomy) of charging at each charge, we obtain this cost.

### 3.3.2. Discount rate

The discount rate recommended by the French government for use in public socio-economic analyses is 4.5% (Quinet, 2014). This discount rate is used to calculate the annuity in the objective function, using the following equation:

$$annuity_{tec} = \frac{DR \times CAPEX_{tec} ((DR \times ct_{tec}) + 1)}{1 - (1 + DR)^{-lt_{tec}}} \quad (25)$$

Where  $DR$  is the discount rate,  $ct_{tec}$  is the construction time,  $lt_{tec}$  is the technical lifetime and  $annuity_{tec}$  is the annualized investment of the technology  $tec$ .

### **3.3.3. Social cost of carbon**

Shirizadeh (2021) concludes that in the EOLES\_mv model using an hourly resolution, carbon-neutrality is reached for a Social Cost of Carbon (SCC) of €200/tCO<sub>2</sub>. Therefore, all the results presented are for this SCC value.

## **3.4. Other limiting constraints and model parametrization**

All the remaining input data (limiting capacity and annual energy supply constraints, model parametrization for the French case for the year 2050 etc.) can be found in Shirizadeh (2021).

## **3.5. Application to time-series aggregation methods**

### **3.5.1. Resolution variation**

For the coarser-resolution versions of EOLES\_mv, the input profiles are prepared by taking an average over the hourly data that are in the considered time-step. Therefore, for a four-hour time-step from the fifth to the eighth hour of the day, an average of the hourly values from these four hours is taken to give the value of the profiles in the time-step under consideration.

### **3.5.2. Representative periods**

To prepare the input data, each day of each week has been categorized as day 1 to 7, then hourly profiles of each input data series have been considered by taking an average over the days of the same category. Therefore, the hourly profiles of each typical day for the representative week for a considered period are the average of all the days with the same category in that period (one month, two months or three months).

## **4. Results**

In this section, we present the results from the optimization with the seven versions of the EOLES\_mv model presented in Sections 2.2 and 2.3 above. In Sections 4.1 to 4.4, we present the results of optimizations applying the time-series aggregation methods, in which the objective function (the social cost) and the other output variables are also calculated applying these methods. In Section 4.5, we optimize the capacity mix based on one time-series aggregation method and then we optimize the dispatch at hourly resolution, to assess the extra cost of this sub-optimal capacity mix, when applied to hourly data.

### **4.1. Energy mix**

For electricity-generating technologies and gas (offshore and onshore wind, solar PV, run-of-river, dams & reservoirs and nuclear energy), we present the amount of electricity generated. For natural (fossil) gas, methanization (anaerobic digestion of organic waste) and pyro-gasification of biomass, we present the thermal energy of natural gas. These primary energy vectors can be either used directly to satisfy the final energy demand, or converted to other energy forms (heat, natural gas,



electricity and hydrogen) to form secondary energy vectors. For both primary and secondary energy vectors, storage possibilities can also allow the energy to be stored for later use.

Figures 2 and 3 show the energy mix for both time-series aggregation methods: resolution variation (hourly, two-hourly, four-hourly and eight-hourly temporal resolutions) and representative periods (hourly continuous case and the versions with representative weeks over one, two and three months). Note that Figures 2.a and 3.a are identical since both present the results with hourly resolution over a full year. For nuclear energy, the values in these figures show the electricity generated and do not include the waste heat generated in the process.

In addition, Appendix 2 and 3 present the installed capacities and annual energy production for both time-series aggregation methods. Since the optimal energy mix (with hourly resolution) includes around 80 GW of solar PV and the same amount of onshore wind, the generation profile varies massively from one hour to the other, especially during the morning and the afternoon<sup>1</sup>.

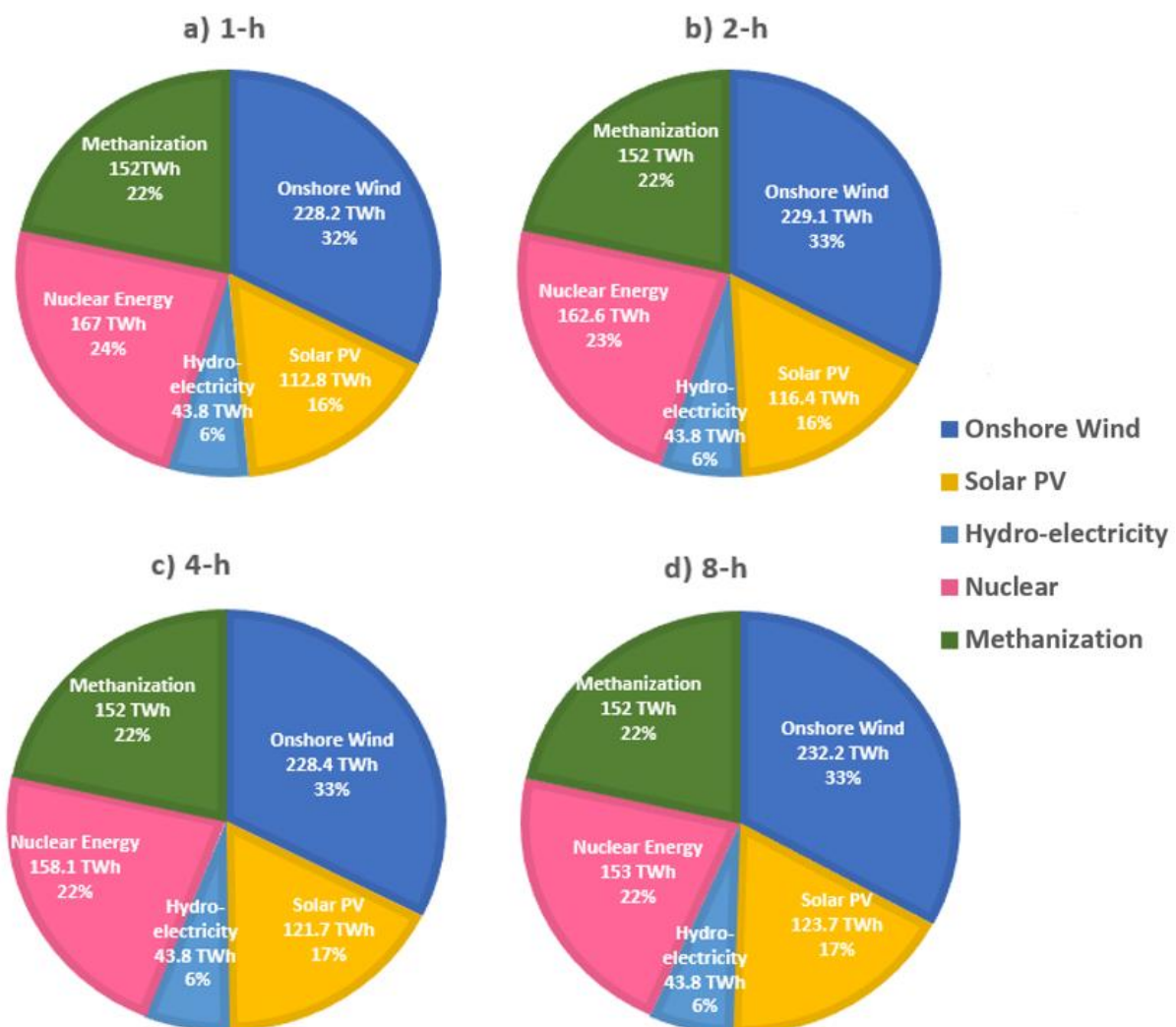


Figure 2. Annual energy supply from each supply technology for different temporal resolutions. These values are in  $TWh_e$  for nuclear power, offshore and onshore wind power, solar PV and hydroelectricity, and in  $TWh_{th}$  for methanization.

<sup>1</sup> Cf. Figure 2 in Shirizadeh et al., 2022, which presents the hourly profile for two typical weeks, for the EOLES\_elecRES model. The method to generate the VRE profiles is the same as in the present paper, so the hourly generation profile is similar.

In the model with an hourly resolution over the whole year (Figure 2.a), the primary energy is mostly in the form of electricity (78% for all temporal resolutions) and this electricity is mainly (71%) from renewable sources. The only primary energy supply technology providing energy in the form of gas is methanization: no fossil gas is used, the explanation being that it is too costly due to the relatively high SCC value (€200/t CO<sub>2</sub>).

All the three coarser resolution versions (Figure 2b, 2c and 2d) provide almost identical results. The contribution from renewables increases slightly, replacing 14TWh<sub>e</sub>/year of nuclear energy. This increase is mainly led by Solar PV. A likely explanation is that PV variability decreases by lowering the temporal resolution of the model. However, the energy mix for the eight-hourly temporal resolution remains very similar to the energy mix with one-hourly temporal resolution.

The energy production from methanization is the same for all the temporal resolutions, and it is the upper bound of energy that can be produced from this technology (152TWh<sub>th</sub>/year). The same is true for hydroelectricity.

On the contrary, for representative periods, the energy mix shows a very wide deviation from the base case that gives continuous representation of a year.

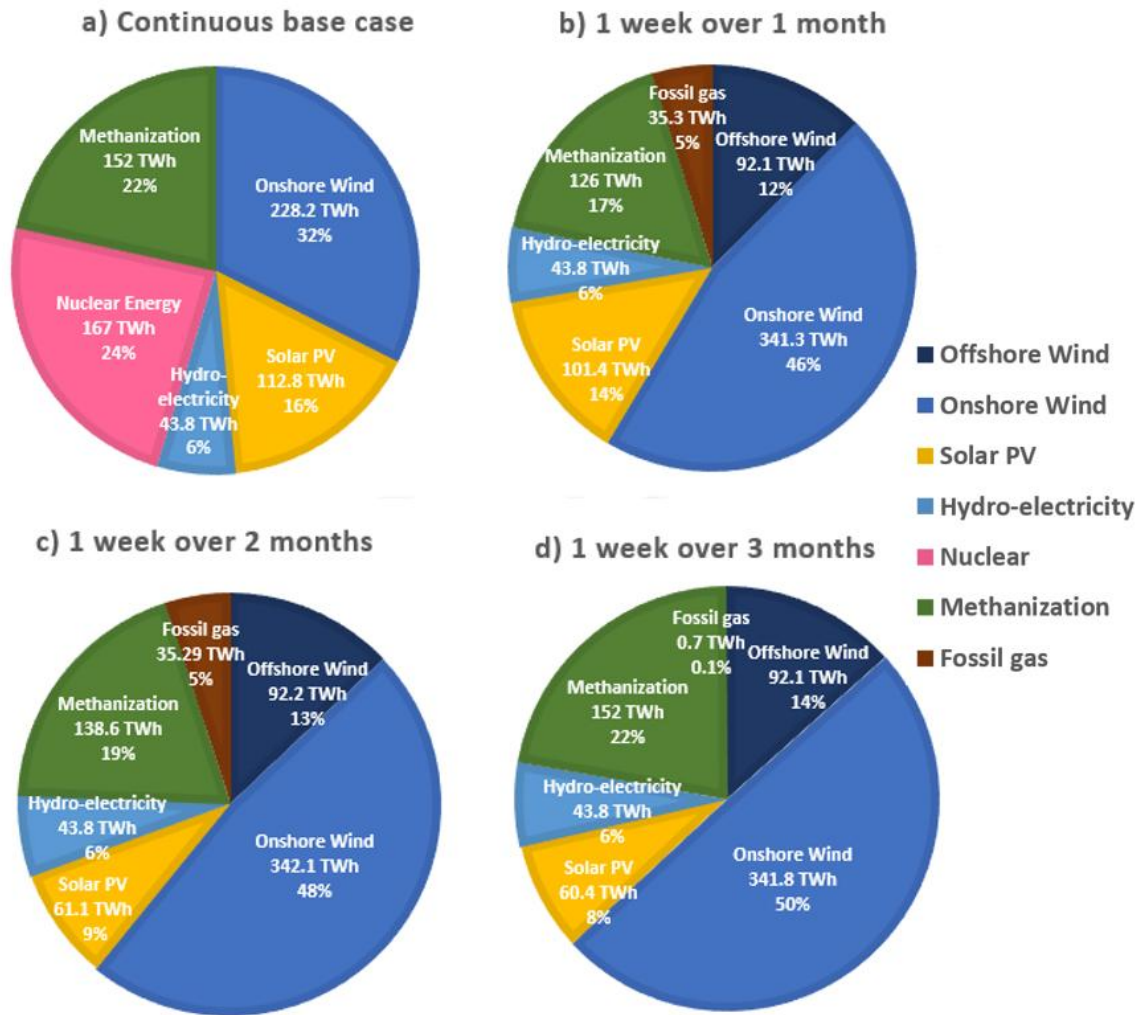


Figure 3. Annual energy supply from each primary supply technology for different representative period selections. These values are in  $TWh_e$  for nuclear power, offshore and onshore wind power, solar PV and hydroelectricity, and in  $TWh_{th}$  for methanization and fossil gas.

Nuclear power (initially 24% of primary energy supply) disappears completely from the energy supply side, while offshore wind and fossil gas are now part of the mix (12% to 13% and up to 5% of the energy supply respectively). The contribution of onshore wind energy to the primary energy supply increases from 32% in the base case to 50% for the case with one representative week over three months. A likely explanation is that representative week selection decreases the variability of weather, reducing one of the main drawbacks of wind power: the large variation of the capacity factor within a year.

To compare the error caused by each time-series aggregation method, we calculate the mean absolute percentage error (MAPE) which represents the average error when several variables are considered together (Figure 4). Here the mean absolute percentage error of annual energy production from offshore and onshore wind, solar PV, nuclear power, methanization, hydroelectricity, pyro-gasification of biomass and fossil gas is considered, and it is calculated by

summing the normalized absolute differences over these technologies<sup>1</sup> and dividing it by the number of technologies considered:

$$MAPE = \frac{1}{n} \sum_{i=1}^n \left| \frac{x_i - x_i^*}{x_i^*} \right| \quad (26)$$

Where  $x_i$  is the annual energy production of each technology  $i$  for each temporal resolution,  $x_i^*$  is the annual energy production of that technology for the case with hourly temporal resolution and  $n$  is the number of technologies considered.

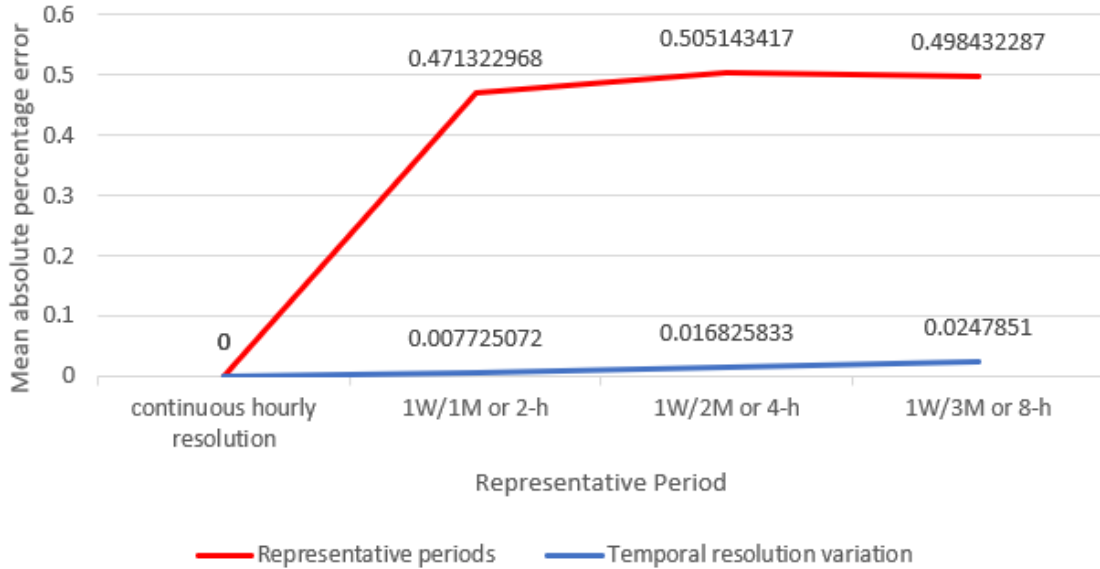


Figure 4. Mean absolute percentage errors in installed capacity for each time-series aggregation method compared to the base case (continuous hourly temporal resolution over a full year)

The MAPE for any of the coarser-than-hourly temporal resolutions studied is negligible compared to that of the representative week selection method. The former increases from 0.0077 (0.77%) for the two-hourly resolution to 0.0248 (2.48%) for the eight-hourly resolution, while with the representative week selection method the MAPE is around 0.5 (50%) for the three representative week selection periods. Interestingly, the MAPE barely improves when the number of weeks increases, from one week per three month (hence four weeks at hourly resolution) to one week per month (hence twelve weeks at hourly resolution).

## 4.2. Electricity mix

Since the literature highlights the importance of temporal resolution in power system modelling with a large proportion of wind and PV, it is worth focusing on the electricity mix. Figures 5 and 6 show the electricity mix and its role in satisfying final energy demand for different sectors, for each of the studied time-series aggregation methods.

<sup>1</sup> The installed capacity of hydroelectricity is fixed, and pyro-gasification of biomass never appears in the optimal mix for the social cost of carbon that we consider.

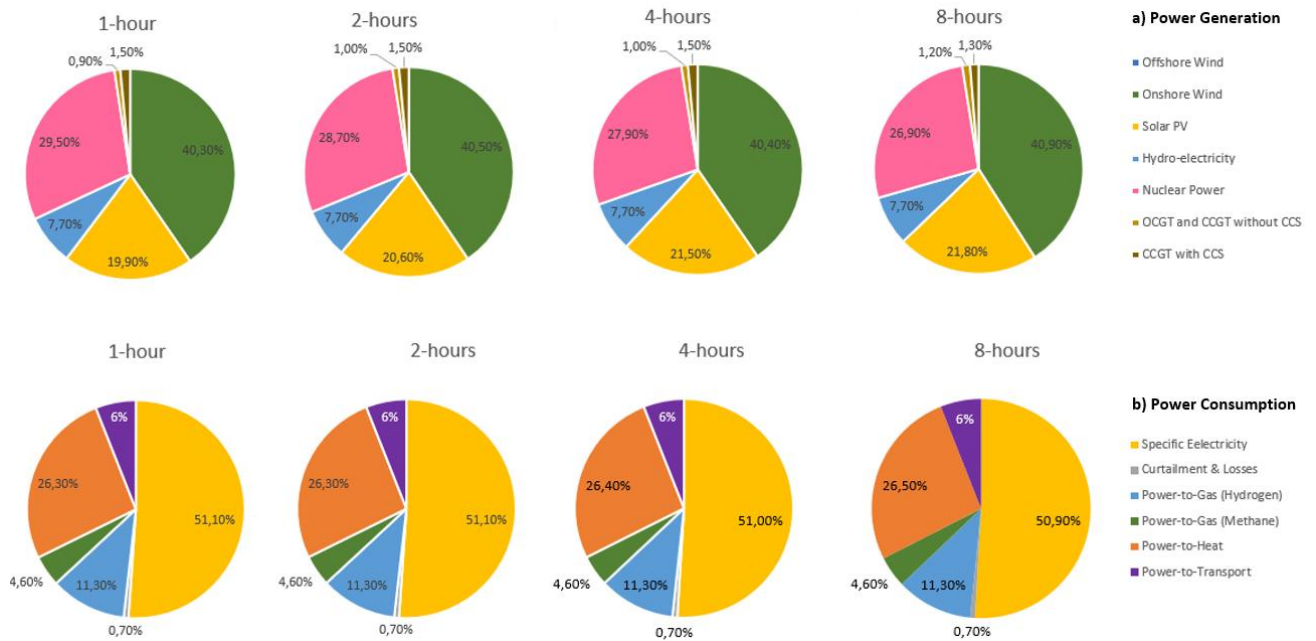


Figure 5. Annual electricity supply and consumption mix for different temporal resolutions

The electricity supply and consumption mixes remain nearly stable across different temporal resolutions (Figure 5). As this temporal resolution becomes coarser, the contribution of nuclear power to the electricity supply decreases slightly from 29.5% to 26.9%, and it is partially replaced by solar PV and onshore wind power (from 19.9% to 21.8% and from 40.3% to 40.9% respectively). The electricity consumption side remains nearly the same whatever the temporal resolution.

Electricity supply for different representative weeks is very different from the continuous base case (Figure 6). For representative week modelling, nuclear power is eliminated, while both onshore and offshore wind power technologies reach their maximal installation limits (120GW and 20GW) and they provide a very large proportion of the electricity supply (from 73.6% to 80.7%). Increasing the length of the represented period reduces the contribution of solar power to the electricity supply from 19.9% in the base case to 10.7% in the case with one representative week over three months. Therefore, nuclear energy and (to a lesser extent) solar PV are replaced by offshore and onshore wind power. Besides, as the variability of wind and solar production decreases with representative weeks, so does the need for dispatchable OCGT and CCGT (with and without CCS). From the base case with continuous time-series to the case with one representative week over three months, the contribution of these gas turbines to the electricity supply decreases from 2.5% to 0.4%.

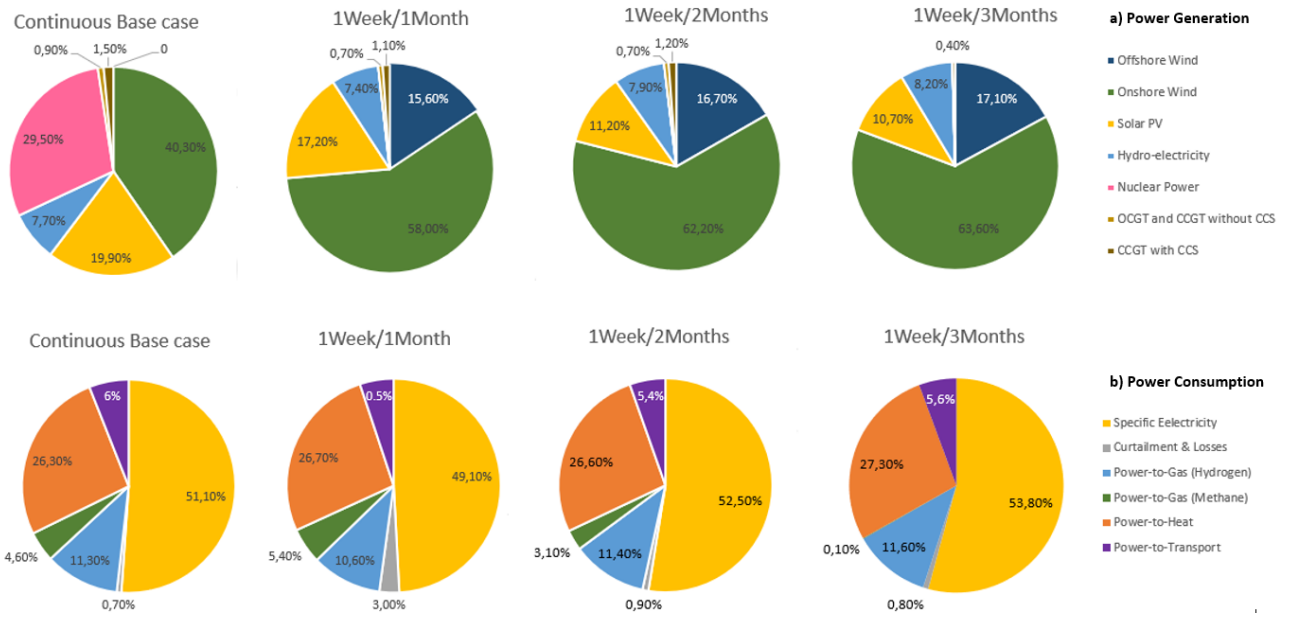


Figure 6. Annual electricity supply and consumption for different representative periods

For representative periods, the difference in electricity consumption from the continuous base case is larger than in the cases where temporal resolution is varied. However, it remains marginal: the already small proportion of electric vehicles in light transport disappears as the represented period grows and the only use of electricity in the transport sector is for rail (30TWh<sub>e</sub>/an). To sum up, relying on representative periods has massive impacts on the electricity mix in terms of both supply and consumption.

### 4.3. Cost and emissions

Table 6 shows the annualized cost of the energy system, CO<sub>2</sub> emissions from the energy system, the calculation time of the EOLES\_mv model for different temporal resolutions, and the difference from the case with hourly temporal resolution.

Table 6. Simulation time, cost and CO<sub>2</sub> emissions for different temporal resolutions and their difference from the base case of hourly resolution<sup>1</sup>

Main characteristics	Temporal Resolution						
	1-h	2-h	Difference*	4-h	Difference*	8-h	Difference*
Total simulation time (s)	216 254	19 974	-90.8%	3 180	-98.5%	339	-99.8%
LP generation time (s) <sup>2</sup>	210	84	-60%	8	-96.2%	2	-99.1%
CPLEX solution time (s) <sup>3</sup>	216 044	19 890	-90.8%	3 172	-98.5%	337	-99.8%
Annual social cost of the energy system (€bn./year) **	59.55	59.51	-0.07%	59.43	-0.20%	59.39	-0.27%
Annual CO <sub>2</sub> emissions (MtCO <sub>2</sub> /year)	-2.51	-2.43	-3.19%	-2.37	-5.58%	-2.19	-12.75%

\* Difference from the 1-h resolution model.

\*\* The technical cost includes the annualized fixed cost and the variable cost. In addition, the social cost includes the value of CO<sub>2</sub> emissions, evaluated at the social cost of carbon (€200/t CO<sub>2</sub>).

Changing the temporal resolution from one hour to two hours leads to a nearly 11-fold decrease in calculation time, with an error of less than 0.1% in the annualized cost of the energy system. As this temporal resolution becomes coarser, the calculation time becomes even smaller (a 640-fold reduction in calculation time for the case with eight-hour temporal resolution), while the cost-related error only reaches 0.27%. While the error in CO<sub>2</sub> emissions (which are negative whatever the temporal resolution) is higher in percentage terms, it remains very low in absolute terms (at most 0.32 MtCO<sub>2</sub>/year). The social cost is slightly lower with coarser-than-one-hour resolutions because by averaging two (or four, or eight), adjacent time-steps, we reduce the peak residual demand (i.e. the difference between electricity demand and variable renewable energy generation) hence the need for storage and dispatchable power.

Representative period selection also provides a huge reduction in calculation time; one representative week over one month leads to a nearly 250-fold reduction in the overall simulation time (Table 7). This gain lies between that produced by the 4-hour and 8-hour resolution simulations presented above. However, the difference in cost and emissions is not negligible. The error in the estimation of the energy system cost is much higher than for the resolution variation methods, varying from 4.7% to 10.1%. Because of the proportion of fossil gas in the primary energy supply, emissions become positive for the cases of one week over one and two months.

<sup>1</sup> The computer used for these simulations has 128 GB of RAM and its CPU is an Intel® Xeon® Bronze 3106 with 8 cores at 1.7 GHz.

<sup>2</sup> Time required for the modelling software (GAMS) to load all the input data, identify different variables and equations, and make the link between the sets, parameters, variables and equations.

<sup>3</sup> Time required for the CPLEX solver to solve the linear optimization problem.

Table 7. Simulation time, cost and CO<sub>2</sub> emissions for different representative periods and their difference from the base case of hourly resolution for a continuous period of one year

Main characteristics	Representative periods						
	Base	1W/1M	Difference*	1W/2M	Difference*	1W/3M	Difference*
Total simulation time (s)	216 254	869.5	99.6%	161.4	99.93%	61	99.97%
LP generation time (s)	210	8.3	96.05%	2.3	98.9%	1.4	99.33%
CPLEX solution time (s)	216 044	861.2	99.6%	159.1	99.93%	59.6	99.97%
Annual social cost of the energy system (€bn./year) **	59.55	56.76	4.69%	55.665	6.52%	53.565	10.05%
Annual CO <sub>2</sub> emissions (MtCO <sub>2</sub> /year)	-2.51	6.25	349%	6.198	346.93%	-0.401	84.02%

\* Difference from the base case.

\*\* The technical cost includes the annualized fixed cost and the variable cost. In addition, the social cost includes the value of CO<sub>2</sub> emissions, evaluated at the social cost of carbon (€200/t CO<sub>2</sub>).

#### 4.4. Variant case: suppression of nuclear power as a dispatchable power production option

In the previous sections we saw that the results of coarser-than-hourly temporal resolutions are very similar to those with hourly temporal resolution. The contrast between this result and that of pre-existing research based on electricity-only models raises the question of how robust it is. The contrast might be due to the lower quantity of short-term storage in the result of our optimization: battery storage only reaches 5 GW compared to, for example 11 to 16 GW in the central-cost scenario electricity-only optimization presented in Shirizadeh and Quirion (2021), and 20 GW in the 100% renewable optimization presented in Shirizadeh et al. (2022), both articles being based on the EOLES family of models.

In the results presented above, the importance of short-term storage is reduced by sector coupling (which allows curtailment of variable renewable energy production to be reduced) but also by nuclear power, which reaches 20GW and 160TWh<sub>e</sub>/year. The latter is used as a dispatchable electricity source, when variable renewables are not enough to satisfy demand. Nuclear power therefore contributes to reducing the need for storage.

In this section, we present the results for the same temporal resolution reduction methods as above, but with nuclear power removed from the available technologies. Figure 7 shows the primary energy supply mix for the case with no nuclear power.



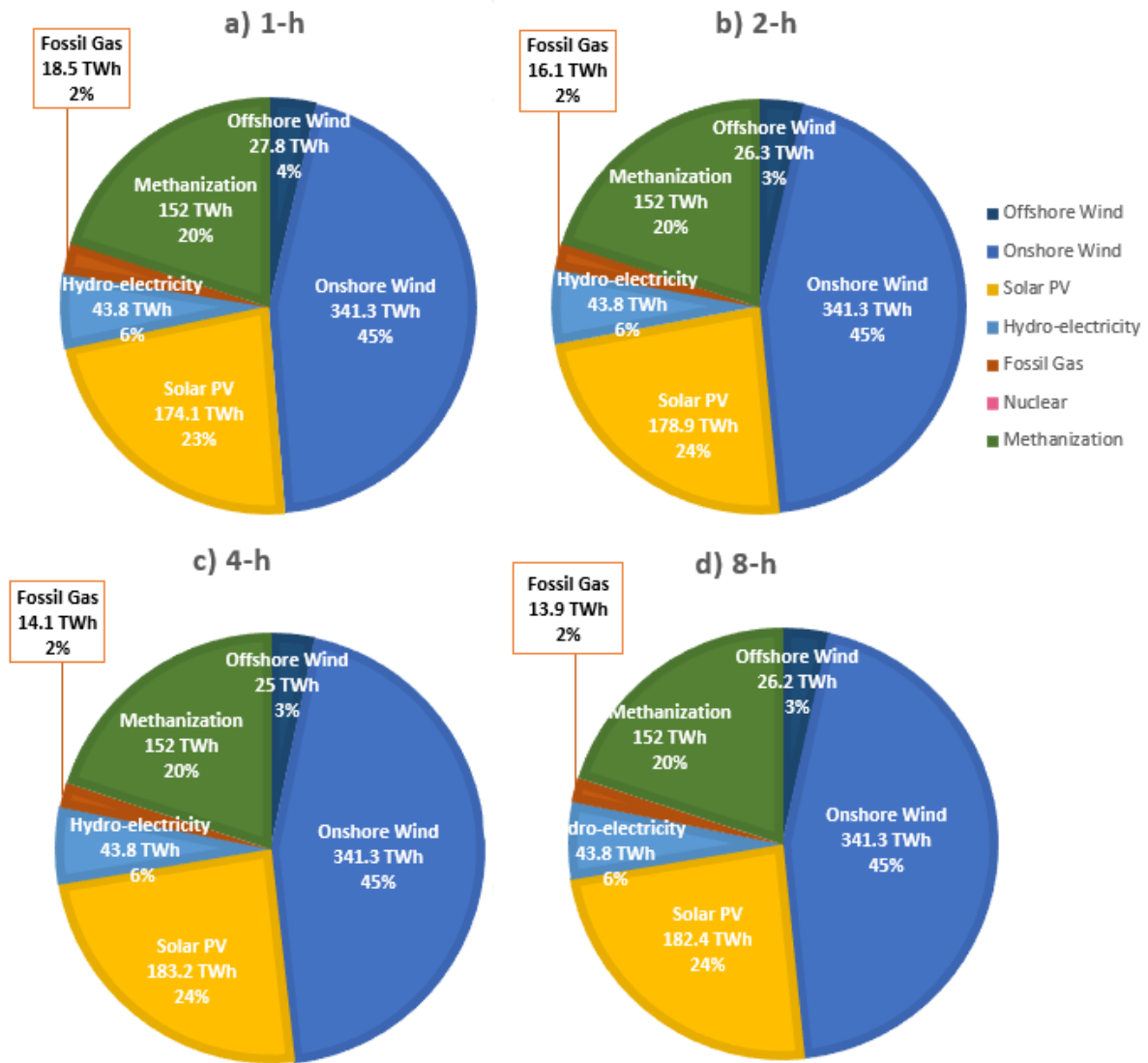


Figure 7. Annual energy supply from each primary supply technology for different temporal resolutions without nuclear power. These values are in  $TWh_e$  for nuclear power, offshore and onshore wind power, solar PV and hydroelectricity, and in  $TWh_{th}$  for methanization and fossil gas.

The proportion of the energy supply technologies remains almost the same for all four temporal resolutions. In the absence of nuclear power, offshore wind appears in the energy mix, varying between 3% and 4% of the primary energy supply (from 25 TWh to 27.8 TWh), and onshore wind is installed to its maximal capacity, producing 341.33 TWh of electricity at all temporal resolutions. The addition of fossil gas can be observed, generating 18.5 TWh for the hourly temporal resolution. By decreasing the resolution from one hour to eight hours, the required flexibility, and thus the fossil gas supply, decreases (from 18.5 TWh to 13.9 TWh).

Figure 8 shows the electricity production and consumption for simulations with different temporal resolutions (without nuclear power).

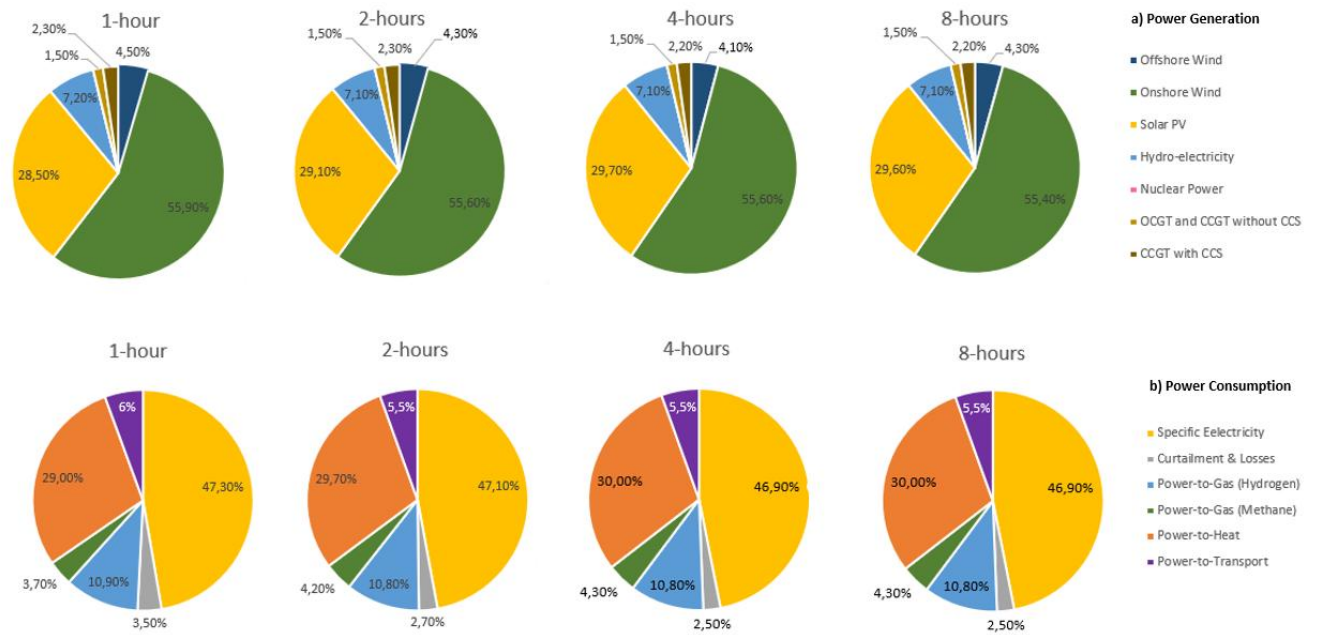


Figure 8. Annual electricity supply and consumption mix for different temporal resolutions in the absence of nuclear power

Electricity production and consumption remain nearly identical among the various temporal resolutions. The largest error is a 1.2% increase in the proportion of solar PV. On the consumption side, all the end-uses keep the same energy consumption from electricity. A slight increase in methanation from 3.7% to 4.3% leads to a slight decrease in curtailment and other losses (from 3.5% to 2.5%). However, even for a temporal resolution of eight hours the power system remains nearly identical compared to the optimization with hourly temporal resolution.

Similarly, Table 8 compares the cost and the emissions at each temporal resolution. As can be seen, when the model uses an eight-hour temporal resolution, the cost is only 0.35% lower than with hourly temporal resolution. Similarly, annual CO<sub>2</sub> emissions are almost nil in every case, varying between 0.04MtCO<sub>2</sub>/year and -0.74MtCO<sub>2</sub>/year.

Table 8. Cost and emissions resulting from modelling with hourly temporal resolution and coarser-than-hourly temporal resolutions for the case with no nuclear power

Main characteristics	Temporal Resolution						
	1-h	2-h	Difference	4-h	Difference	8-h	Difference
Annual social cost of the energy system (€bn/year) *	60.16	60.10	0.10%	59.99	0.28%	59.95	0.35%
Annual CO <sub>2</sub> emissions (MtCO <sub>2</sub> /year)	0.04	-0.37	-	-0.69	-	-0.74	-

\* The technical cost includes the annualized fixed cost and the variable cost. In addition, the social cost includes the value of CO<sub>2</sub> emissions, evaluated at the social cost of carbon (€200/t CO<sub>2</sub>).

Thus coarser-than-hourly temporal resolutions remain very accurate while drastically reducing the calculation time, even when a major low carbon dispatchable energy supply technology is eliminated. Appendix 5 shows installed capacities and annual energy production for each technology.

#### 4.5. The extra cost of optimizing capacities based on a coarse temporal resolution

In the previous sections, we showed that the error values of modelling with a time resolution coarser than one hour are negligible, while the gains in computational tractability are very high.

Therefore, modelling with coarser temporal resolution seems to provide an attractive trade-off between precision and calculation time.

However, if generation and storage capacities are optimized based on a coarser-than-hourly temporal resolution, shortages in energy supply may occur during parts of the resulting longer periods between data points. For instance, supply may match demand over two hours considered as a whole, but not over each of these two hours considered separately. The value of these shortages may be assessed through an assumed value of lost load. Therefore, the aim of this section is to assess the extra cost of optimizing generation and storage capacities based on coarser-than-hourly temporal resolutions, when the dispatch of these capacities is optimized with an hourly temporal resolution<sup>1</sup>.

To address this question, we run the hourly model with the installed capacities of the energy supply, conversion and storage technologies obtained by the optimizations with coarse temporal resolutions, and we define a value of lost load of €10,000/MWh<sub>e</sub> for electricity supply (Gils, 2014). We saw previously that using an SCC of €200/tCO<sub>2</sub> and with nuclear power allowed, fossil gas is eliminated from the optimal mix. Since this may change when dispatch is optimized on a finer resolution than investment, we present two cases.

The first case aims to limit the extra cost from lost load by allowing fossil gas imports, and thus potentially positive CO<sub>2</sub> emissions. The cost, CO<sub>2</sub> emissions and lost electricity load are presented in Table 9.

Table 9. Social and technical costs, lost load and CO<sub>2</sub> emissions with the installed capacities optimized at coarse temporal resolution and dispatch optimized at hourly resolution, with the ability to import fossil gas

	1-h	2-h	4-h	8-h			
<b>Annual social cost of the energy system (€bn./year) *</b>	59.55	59.57	+0.03%	59.88	+0.55%	59.70	+0.25%
<b>Annual technical cost of the energy system (€bn./year) *</b>	60.05	60.05	+0%	59.61	-0.73%	60.03	-0.03%
<b>Lost Load (GWh<sub>e</sub>/year)</b>	0	0		3.77		10.03	
<b>Lost load (percentage of entire electricity load)</b>	0	0		0.0007%		0.0019%	
<b>Fossil gas consumption (TWh<sub>th</sub>/year)</b>	0	0.101		15.9		2.72	
<b>CO<sub>2</sub> emissions (MtCO<sub>2</sub>/year)</b>	-2.51	-2.42		1.33		-1.68	

\* The technical cost includes the annualized fixed cost and the variable cost. In addition, the social cost includes the value of lost load and the value of CO<sub>2</sub> emissions, evaluated at the social cost of carbon (€200/t CO<sub>2</sub>).

Although the extra cost is very limited (between €0.02bn./year and €0.15bn./year), the CO<sub>2</sub> emissions differ (especially for the 4-hourly resolution), because a small proportion of the primary energy is provided by fossil gas (up to 15.9TWh<sub>th</sub>/year for the 4-hourly temporal resolution, i.e. 2% of electricity generation). In every case, the lost load is very small: at most 10GWh<sub>e</sub>/year for the 4-hourly temporal resolution (0.0019% of the load).

<sup>1</sup> As we have seen, the capacities optimized using the representative period selection method are very different from those optimized using the continuous, hourly base case. Thus, it is obvious that optimizing the dispatch of those capacities over a continuous, hourly period would lead to a large extra cost, so we do not assess this case.

The importation of fossil gas is the reason why the CO<sub>2</sub> emissions slightly increase from the hourly temporal resolution case (France has no longer any fossil gas resources). Keeping the emissions below zero would require importation of fossil gas to be limited to its value resulting from the optimization with hourly temporal resolution (i.e. zero). Table 10 shows the same results as in Table 9, but for the second case, with no ability to import fossil gas.

Table 10. Social and technical costs, lost load and CO<sub>2</sub> emissions with the installed capacities optimized at coarse temporal resolution and dispatch optimized at hourly resolution, with no ability to import fossil gas

	1-h	2-h		4-h		8-h	
<b>Social cost (bn.€/year)</b>	59.55	59.57	+0.03%	60.97	+2.38%	59.79	+0.4%
<b>Technical cost (bn.€/year)</b>	60.05	60.05	+0%	61.46	+2.34%	60.23	+0.3%
<b>Lost load (GWh<sub>e</sub>/year)</b>	0	0		3.77		10.03	
<b>Lost load (percentage of entire electricity load)</b>	0	0		0.0007%		0.0019%	
<b>CO<sub>2</sub> emissions (MtCO<sub>2</sub>/year)</b>	-2.51	-2.43		-2.44		-2.19	

CO<sub>2</sub> emissions remain very close to the 1-hour case, which is expected since the fossil gas import capacity is fixed. The small variation is explained by a small change in BECCS. Although the extra cost is higher than in the previous case, it remains very low based on the 2-hourly resolution: less than 0.03%. The maximal value is for a four-hourly temporal resolution with an extra cost of €1.42bn/year, which remains reasonable (+2.4%).

## 5. Results, discussion and conclusion

Modelling energy systems covering the main energy sectors and the main energy supply, carrier and storage options with high temporal resolution over a full year is computationally demanding. Time-series aggregation methods can reduce the calculation time of energy system models, but the trade-off between computational tractability and accuracy in the optimal allocation of different options in an energy system model with sector coupling had yet to be analyzed – unlike the case of electricity-only models, which has been analyzed in depth.

In this paper, we have applied the two main time-series aggregation methods (temporal resolution reduction and representative period selection) to an energy system model with sector coupling, in order to test their benefit (in terms of reduced simulation time) and cost (in terms of output inaccuracy). The results are clear: while both methods massively reduce the calculation time, the accuracy of the representative period selection method is low while that of the temporal resolution reduction method is very high.

The inaccuracy of the representative period selection is seemingly caused by the implied reduction in weather (especially wind) variability over time, which leads to a higher proportion of wind power and to a lower cost. This is consistent with the findings by Alimou et al. (2020); by comparing TIMES-FR (a model optimizing dispatch and investment with representative weeks) and ANTARES (a dispatch model developed by RTE, the French transmission network operator, with hourly temporal resolution) they show that the former underestimates the system cost by 28% and that the capacity mix derived from TIMES-FR does not meet the supply/demand adequacy requirements of the French public authorities (i.e. annual loss of load of no more than three hours).

The accuracy of the resolution variation method is more puzzling: even moving from hourly to eight-hourly resolution has almost no impact on the energy mix, energy system cost, emissions and load curtailment. Moreover, this result stands irrespective of the inclusion of nuclear power among the generation technologies – without which the energy mix is 98% renewable. A less than 2.5% mean absolute percentage error for the primary energy mix and less than 0.3% variation in the energy system cost seems an acceptable price to pay for a 640-fold reduction in calculation time using eight-hourly resolution. This result is especially noticeable since the intra-day variability of wind and especially PV is high, and the installed capacities in these technologies are large (around 80 GW each if nuclear is part of the mix, around 120 GW each if not). Therefore we can expect that in a similar model with less PV, coarser-than-hourly resolution would generate even less discrepancies.

Why is the resolution variation method more accurate for a model with sector coupling such as the one used here, compared to an electricity-only model? We suspect that the reason is the relatively low curtailment (~3%) and the very low short-term storage requirement permitted by sector coupling. With the same model without sector coupling, around 10 to 15% of electricity is curtailed and batteries are used as a short-term storage option (Shirizadeh et al., 2022; Shirizadeh and Quirion, 2021). In such an electricity-only model, reducing temporal resolution would decrease energy losses through storage and curtailment. Therefore, it would reduce the total cost and change the energy mix significantly.

Coarser-than-hourly temporal precision would allow future modelling studies to increase their computational tractability, maintaining the required precision in calculations with much faster solution time. In those circumstances, other aspects of energy system modelling could be developed, such as better technical representation of different technologies, inclusion of a greater number of options in the modelling and application of detailed sensitivity and robustness studies that require wide ranges of scenarios to account for the uncertainties regarding energy demand, technology costs, resource availability and weather variability.

Comparing both methods for other energy system optimization models featuring sector coupling would be welcome to confirm the external validity of our results. In the meantime, we highlight that the key features of our model are similar to that of other well-known such models, such as PyPSA-*eur-sec-30* (Brown et al., 2018a): both use linear optimization to minimize annual operational and investment costs subject to physical constraints, assuming perfect foresight, and both use wind and PV generation profiles based on weather data and downscaling methods. The set of technologies represented is also very close. The main differences are that the choice between gas and electricity for transport is endogenous in *EOLES\_mv* and that *PyPSA-*eur-sec-30** features several nodes, but we do not see why these differences would change our results concerning the relative performance of the two time-series aggregation methods.

Our representative week choice is based on preparation of an average week for each month, without considering other grouping characteristics of different periods. One interesting extension of this work could be the choice of representative periods based on similar weather and demand characteristics, which might improve the performance of representative period selection, such as seasonal representative periods.

Similarly, the coarser-than-hourly time-slices are based on simple division of 24 hours of a day to two-hour, four-hour and eight-hour long time-steps with no particular consideration of variable time-step choice for a day as we did previously for an electricity-only model (De Guibert et al., 2020). The performance of the resolution variation methods could be improved by smarter sub-sampling of daily time-steps.

However, even without variable time-step choice, this method performs very well with negligible error compared to modelling with hourly temporal resolution. If this positive result is confirmed for other models, it could allow modelling teams to benefit from the computer resources which are saved by this coarser time resolution, e.g. to analyze more complex models and richer sets of scenarios.

## References

- ADEME (2015). *Vers un mix électrique 100 % renouvelable*. ISBN : 979-10-297-0475-8.
- ADEME (2017). *Actualisation du scénario énergie-climat ADEME 2035-2050*. ISBN: 979-10-297-0921-0.
- ADEME (2018). *Mix de gaz 100% renouvelable en 2050?* ISBN: 979-10-297-1047-6
- Alimou, Y., Maïzi, N., Bourmaud, J. Y., & Li, M. (2020). Assessing the security of electricity supply through multi-scale modeling: The TIMES-ANTARES linking approach. *Applied Energy*, 279, 115717.
- Brown, T., Schlachtberger, D., Kies, A., Schramm, S., & Greiner, M. (2018a). Synergies of sector coupling and transmission reinforcement in a cost-optimized, highly renewable European energy system. *Energy*, 160, 720-739.
- Brown, T. W., Bischof-Niemz, T., Blok, K., Breyer, C., Lund, H., & Mathiesen, B. V. (2018b). Response to 'Burden of proof: A comprehensive review of the feasibility of 100% renewable-electricity systems'. *Renewable and Sustainable Energy Reviews*, 92, 834-847.
- CGDD (2017). *Analyse coût bénéfice des véhicules électriques*, 2017. Commissariat générale du développement durable.
- CRE (2018). *Observatoire des marchés de détail de l'électricité et du gaz naturel du 3e trimestre 2018*. CRE, Paris
- De Guibert, P., Shirizadeh, B., & Quirion, P. (2020). Variable time-step: a method for improving computational tractability for energy system models with long-term storage. *Energy*, 119024. <https://doi.org/10.1016/j.energy.2020.119024>
- DGEC (2019). *Synthèse du scénario de référence de la stratégie française pour l'énergie et le climat*. Direction générale de l'énergie et du climat. 15/03/2019
- Doudard, R. (2018). *Flexibilité et interactions de long terme dans les systèmes multi-énergies: analyse technico-économique des nouvelles filières gazières et électriques en France* (Doctoral dissertation, Paris Sciences et Lettres).
- ENEA (2016). De Bucy, J., Lacroix, O., & Jammes, L. (2016). *The potential of Power-to-Gas*. ENEA Consulting, Paris, France.
- ENTSO-E (2013). *Network Code on Load-Frequency Control and Reserves* 6, 1–68.
- FCH JU (2015). *Commercialization of energy storage in Europe: Final report*.
- Gea-Bermúdez, J., Jensen, I. G., Münster, M., Koivisto, M., Kirkerud, J. G., Chen, Y. K., & Ravn, H. (2021). The role of sector coupling in the green transition: A least-cost energy system development in Northern-central Europe towards 2050. *Applied Energy*, 289, 116685.
- Gils, H. C. (2014). Assessment of the Theoretical Demand Response Potential in Europe. *Energy*, 02019. <https://doi.org/10.1016/j.energy.2014.02.019>.

Henning, H. M, Palzer, A. (2014). A comprehensive model for the German electricity and heat sector in a future energy system with a dominant contribution from renewable energy technologies—Part I: Methodology. *Renewable and Sustainable Energy Reviews*, 30, 1003-1018.

Hoffmann, M., Kotzur, L., Stolten, D., & Robinius, M. (2020). A Review on Time Series Aggregation Methods for Energy System Models. *Energies*, 13(3), 641.

IEA (2019). *World Energy Outlook 2019*, Paris, France: OECD/IEA.

JRC (2014) *Energy Technology Reference Indicator Projections for 2010–2050*. EC Joint Research Centre Institute for Energy and Transport, Petten.

JRC (2017) *Cost development of low carbon energy technologies - Scenario-based cost trajectories to 2050*, EUR 29034 EN, Publications Office of the European Union, Luxembourg, 2018, ISBN 978-92-79-77479-9, doi: 10.2760/490059, JRC109894.

Kang, S., Selosse, S., & Maïzi, N. (2017). Is GHG mitigation policy enough to develop bioenergy in Asia: a long-term analysis with TIAM-FR. *International Journal of Oil, Gas and Coal Technology*, 14(1-2), 5-31.

Krakowski, V., Assoumou, E., Mazauric, V., & Maïzi, N. (2016). Reprint of Feasible path toward 40–100% renewable energy shares for power supply in France by 2050: A prospective analysis. *Applied energy*, 184, 1529-1550.

Loisel, R., Alexeeva, V., Zucker, A., & Shropshire, D. (2018). Load-following with nuclear power: Market effects and welfare implications. *Progress in Nuclear Energy*, 109, 280-292.

Lund, H., Østergaard, P. A., Connolly, D., & Mathiesen, B. V. (2017). Smart energy and smart energy systems. *Energy*, 137, 556-565.

NégaWatt (2017). *Scénario négaWatt 2017-2050*.  
[https://negawatt.org/IMG/pdf/synthese\\_scenario-negawatt\\_2017-2050.pdf](https://negawatt.org/IMG/pdf/synthese_scenario-negawatt_2017-2050.pdf)

Perrier, Q. (2018). The second French nuclear bet. *Energy Economics*, 74, 858-877.

Pfenninger, S. & Staffell, I. (2016). Long-term patterns of European PV output using 30 years of validated hourly reanalysis and satellite data. *Energy* 114, pp. 1251-1265.

Pfenninger, S. (2017). Dealing with multiple decades of hourly wind and PV time series in energy models: A comparison of methods to reduce time resolution and the planning implications of inter-annual variability. *Applied Energy*, 197, 1-13.

Postic, S., Selosse, S., & Maïzi, N. (2017). Energy contribution to Latin American INDCs: Analyzing sub-regional trends with a TIMES model. *Energy Policy*, 101, 170-184.

Prina, M. G., Casalicchio, V., Kaldemeyer, C., Manzolini, G., Moser, D., Wanitschke, A., & Sparber, W. (2020). Multi-objective investment optimization for energy system models in high temporal and spatial resolution. *Applied Energy*, 264, 114728.

Quinet, E. (2014). *L'évaluation socioéconomique des investissements publics* (No. Halshs 01059484). HAL.



Samsatli, S., Staffell, I., & Samsatli, N. J. (2016). Optimal design and operation of integrated wind-hydrogen-electricity networks for decarbonising the domestic transport sector in Great Britain. *international journal of hydrogen energy*, 41(1), 447-475.

Schill, W. P. & Zerrahn, A. (2018). Long-run power storage requirements for high shares of renewables: Results and sensitivities. *Renewable and Sustainable Energy Reviews*, 83, 156-171.

Schmidt, O., Melchior, S., Hawkes, A., Staffell, I. (2019). "Projecting the Future Levelized Cost of Electricity Storage Technologies." *Joule* ISSN 2542-4351.

Shirizadeh, B. (2021). Relative role of electricity and gas in a carbon-neutral future: insights from an energy system optimization model. In *Energy, COVID, and Climate Change*, 1st IAEE Online Conference, June 7-9, 2021. International Association for Energy Economics.

Shirizadeh, B., Perrier, Q. & Quirion, P. (2022). How sensitive are optimal fully renewable systems to technology cost uncertainty? *The Energy Journal*, Vol 43. No 1.

<https://doi.org/10.5547/01956574.43.1.bshi>

Shirizadeh, B., & Quirion, P. (2021). Low-carbon options for the French power sector: What role for renewables, nuclear energy and carbon capture and storage?. *Energy Economics*, 95, 105004.

Staffell, I. & Pfenninger, S. (2016). Using Bias-Corrected Reanalysis to Simulate Current and Future Wind Power Output. *Energy* 114, pp. 1224-1239.

Van Stiphout, A., De Vos, K., & Deconinck, G. (2017). "The impact of operating reserves on investment planning of renewable power systems." *IEEE Transactions on Power Systems*, 32(1), 378-388.

Victoria, M., Zhu, K., Brown, T., Andresen, G. B., & Greiner, M. (2019). The role of storage technologies throughout the decarbonization of the sector-coupled European energy system. *Energy Conversion and Management*, 201, 111977.

Vogl, V., Åhman, M., & Nilsson, L. J. (2018). Assessment of hydrogen direct reduction for fossil-free steelmaking. *Journal of Cleaner Production*, 203, 736-745.

Zhu, K., Victoria, M., Brown, T., Andresen, G. B., & Greiner, M. (2019). Impact of CO2 prices on the design of a highly decarbonised coupled electricity and heating system in Europe. *Applied energy*, 236, 622-634.

## Data availability

All the versions of the model and the input data are available on GitHub: [https://github.com/BehrangShirizadeh/EOLES\\_mv\\_temp](https://github.com/BehrangShirizadeh/EOLES_mv_temp).

# Appendices

## Appendix 1. The EOLES\_mv model

### A.1.1. Sets and parameters

Table A.1 presents the sets and indices of the EOLES\_mv model and table A.2 the parameters. Throughout the paper, every energy unit (e.g. MWh) or capacity unit (e.g. MW) is expressed in useful form. For instance, some energy is converted from gas to electricity by OCGT. The input energy in MWh is in the gas carrier, therefore the unit is  $MWh_{th}$  and conversion efficiency by OCGT is 45%. The output energy is in  $MWh_e$  equivalent to the value in  $MWh_{th}$  multiplied by 0.45.

Table A.1. Sets and indices of the EOLES\_mv model

Index	Set	Description
$h$	$\in H$	<b>Hour:</b> the number of hours in a year, from 0 to 8759
$d$	$\in D$	<b>Day:</b> The number of days in a year, from 1 to 365
$w$	$\in W$	<b>Week:</b> The number of weeks in a year, from 1 to 52 (the 52 <sup>nd</sup> week accounts for 10 days)
$m$	$\in M$	<b>Month:</b> the twelve months, from January to December
$tec$	$\in TEC$	<b>Technologies:</b> The set of all energy supply, conversion, storage and non-existing carrier technologies (floating offshore, monopile offshore, onshore, PV, river, lake, nuclear, natural gas, methanization, pyro-gasification, OCGT, CCGT, CCGT with CCS, electrolysis, methanation, heat network, resistive heating, electric heat pump, gas heat pump, central boiler, decentralized boiler, heavy EV, light EV, EV bus, train, heavy ICE, light ICE, ICE bus, PHS, battery, gas storage, individual thermal energy storage -ITES- and central thermal energy storage -CTES)
$gen$	$\in GEN \subseteq TEC$	<b>Generation:</b> Energy supply technologies (floating offshore, monopile offshore, onshore, PV, river, lake, nuclear, natural gas, methanization and pyro-gasification)
$elec$	$\in ELEC \subseteq TEC$	<b>Electricity:</b> The technologies providing electricity by supply, conversion or storage (floating offshore, monopile offshore, onshore, PV, river, lake, nuclear, OCGT, CCGT, CCGT with CCS, PHS and battery)
$gas$	$\in GAS \subseteq TEC$	<b>Gas:</b> The technologies providing gas by supply, conversion or storage (natural gas, methanization, pyro-gasification, electrolysis, methanation and gas storage)
$heat$	$\in HEAT \subseteq TEC$	<b>Heat:</b> The technologies providing heat by conversion and storage (heat network, resistive heating, electric heat pump, gas heat pump, central boiler, decentralized boiler, individual thermal energy storage and central thermal energy storage)
$transport$	$\in TRANSPORT \subseteq TEC$	<b>Transport:</b> The technologies that meet different types of transport demand (heavy EV, light EV, EV bus, train, heavy ICE, light ICE and ICE bus)
$gen_{elec}$	$\in ELEGEN \subseteq ELEC$	<b>Electricity supply:</b> The technologies generating electricity (floating offshore, monopile offshore, onshore, PV, river, lake and nuclear)
$gen_{gas}$	$\in GASGEN \subseteq GAS$	<b>Gas supply:</b> Technologies supplying gas (natural gas, methanization and pyro-gasification)
$biogas_{gas}$	$\in BIOGAS \subseteq GAS$	<b>Renewable gas:</b> biogas supply technologies (methanization and pyro-gasification)
$vre$	$\in VRE \subseteq ELEC$	<b>VRE:</b> variable renewable electricity generation technologies (offshore, onshore, PV and run-of-river)
$str$	$\in STR \subseteq TEC$	<b>Storage:</b> energy storage technologies (PHS, battery, gas storage, individual thermal energy storage and central thermal energy storage)
$str_{elec}$	$\in STRELEC \subseteq ELEC$	<b>Electric storage:</b> technologies providing storage for electricity (battery and PHS)

$str_{gas}$	$\in STRGAS \subseteq GAS$	<b>Gas storage:</b> technologies providing storage for gas (gas storage)
$str_{heat}$	$\in STRHEAT \subseteq HEAT$	<b>Heat storage:</b> technologies providing storage for heat (ITES and CTES)
$conv$	$\in CONV \subseteq TEC$	<b>Conversion:</b> energy vector-change technologies (OCGT, CCGT, CCGT with CCS, electrolysis, methanation, resistive heating, electric heat pump, gas heat pump, central boiler and decentralized boiler)
$conv_{elec}$	$\in CONVELEC \subseteq TEC$	<b>Conversion from electricity:</b> energy vector-change technologies from electricity to other carriers (electrolysis, methanation, resistive heating and electric heat pump)
$conv_{gas}$	$\in CONGAS \subseteq TEC$	<b>Conversion from gas:</b> energy vector-change technologies from gas to other carriers (OCGT, CCGT, CCGT with CCS, gas heat pump, centralized boiler and decentralized boiler)
$central$	$\in CENTRAL \subseteq HEAT$	<b>Central heating:</b> heating technologies needing heat network (electric heat pump, gas heat pump and centralized boilers)
$vector_t$	$\in TVECTOR$	<b>Transport vector:</b> two different engine types for transport sector (EV and ICE)
$cat_t$	$\in TCAT$	<b>Transport category:</b> four categories of transport demand (heavy, light, bus and train)
$ev_{transport}$	$\in EV \subseteq TRANSPORT$	<b>Electric transport:</b> the electric transport technologies (heavy EV, light EV, EV bus and train)
$ice_{transport}$	$\in ICE \subseteq TRANSPORT$	<b>Gas transport:</b> the ICE transport technologies using gas as fuel (heavy ICE, light ICE and ICE bus)
$frr$	$\in FRR \subseteq TEC$	<b>Frequency restoration reserves:</b> Technologies contributing to secondary reserves requirements (lake, PHS, battery, OCGT, CCGT, CCGT with CCS and nuclear)
$co_2$	$\in CO2$	<b>Social cost of carbon scenario:</b> The scenarios are 1, 2, 3, 4, 5 and 6

Table A.2. Parameters of the EOLES\_mv model

Parameter	Unit	Description
$day_h$	[-]	A parameter to show which day each hour is in
$week_h$	[-]	A parameter to show which week each hour is in
$month_h$	[-]	A parameter to show which month each hour is in
$cf_{vre,h}$	[-]	Hourly production profiles of variable renewable energies
$profile_h^{transport}$	[-]	Hourly charging profile of each transport technology
$demand_{heat,h}$	[ $GW_{th}$ ]	Hourly heat demand profile
$demand_{hydrogen,h}$	[ $GW_{th}$ ]	Hourly hydrogen demand profile (for industry)
$demand_{elec,h}$	[ $GW_e$ ]	Hourly electricity demand profile
$demand_h^{heavy}$	[ $Gkm. vehicle$ ]	Hourly transport demand for heavy vehicles
$demand_h^{light}$	[ $Gkm. vehicle$ ]	Hourly transport demand for light vehicles
$demand_h^{bus}$	[ $Gkm. vehicle$ ]	Hourly transport demand for buses
$demand_h^{train}$	[ $GW_{h_e}$ ]	Hourly transport demand for trains (flat)
$lake_m$	[ $GW_{h_e}$ ]	Monthly extractable energy from lakes
$\epsilon_{vre}$	[-]	Frequency restoration requirement because of forecast errors on the production of each variable

		renewable energy
$q_{tec}^{ex}$	[ $GW_e$ ]	Existing installed capacity by each hydroelectric technology
$annuity_{tec}$	[ $M\text{€}/GW/\text{year}$ ]	Annualized capital cost of each technology
$annuity_{str}^{en}$	[ $M\text{€}/GWh/\text{year}$ ]	Annualized capital cost of energy volume for storage technologies
$annuity_{transport}^{vol}$	[ $M\text{€}/GWh/\text{year}$ ]	Annualized capital cost of energy reservoir volume of transport technology
$fO\&M_{tec}$	[ $M\text{€}/GW/\text{year}$ ]	Annualized fixed operation and maintenance cost
$vO\&M_{tec}$	[ $M\text{€}/GWh$ ]	Variable operation and maintenance cost of each technology
$\eta_{str}^{in}$	[-]	Charging efficiency of storage technologies
$\eta_{str}^{out}$	[-]	Discharging efficiency of storage technologies
$\eta_{conv}$	[-]	Conversion efficiency for energy conversion technologies
$\eta_{cat_t}^{vector_t}$	[ $Gkm. vehicle /kWh$ ]	Transport efficiency of each transport technology
$q^{pump}$	[ $GW_e$ ]	Pumping capacity for Pumped hydro storage
$e_{PHS}^{max}$	[ $GWh_e$ ]	Maximum energy volume that can be stored in PHS reservoirs
$g_{biogas}^{max}$	[ $TWh_{th}$ ]	Maximum yearly energy that can be generated from renewable gas supply technologies
$\delta_{uncertainty}^{load}$	[-]	Uncertainty coefficient for hourly electricity demand
$\delta_{variation}^{load}$	[-]	Load variation factor
$r_{nuc}^{up}$	[-]	Maximal ramping up rate of nuclear power
$r_{nuc}^{down}$	[-]	Maximal ramping down rate of nuclear power
$cf_{nuc}$	[-]	The maximal annual capacity factor for nuclear power
$cf_{ocgt}$	[-]	The maximal annuity capacity factor for OCGT plant
$cf_{ccgt}$	[-]	The maximal annual capacity factor for CCGT plant
$cf_{ccgt-ccs}$	[-]	The maximal annual capacity factor for CCGT with CCS plants
$e_{tec}$	[ $tCO_2/GWh$ ]	Emission rate of each technology
$scc_{co_2}$	[ $\text{€}/tCO_2$ ]	Social cost of carbon for each SCC scenario
$\varphi_{CO_2}^{max}$	[ $MtCO_2/\text{year}$ ]	The maximal carbon dioxide that can be stored annually
$\gamma_{methanization}^{CO_2}$	[-]	The green $CO_2$ available as a byproduct of methanization for methanation
$\tau^{hydrogen}$	[-]	The maximal penetration rate of hydrogen in the gas network

## A.1.2. Variables

The variables resulting from the optimization are presented in table A.3.

Table A.3. Variables of EOLES\_mv model

Variable	Unit	Description
$G_{tec,h}$	GWh	Hourly energy generation by technology
$Q_{tec}$	GW	Installed capacity by technology
$STORAGE_{str,h}$	GWh	Hourly energy entering each storage technology (inflow)
$SOC_{str,h}$	GWh	Hourly state of charge of each storage technology (stock)
$S_{str}$	GW	Installed charging capacity by storage technology
$CONVERT_{conv,h}$	GWh	Hourly converted energy by each conversion technology
$CHARGE_{transport,h}$	GWh	Hourly charging of each transport technology
$RESERVOIR_{transport}$	GWh	The energy reservoir volume for each transport technology
$VOLUME_{str}$	GWh	Energy capacity by storage technology
$RSV_{frr,h}$	GW <sub>e</sub>	Hourly upward frequency restoration requirement to manage the variability of renewable energies and demand uncertainties
$COST$	b€	Total energy system cost annualized (minus the investment cost of already installed capacities). This is the objective function to be minimized.

## A.1.3. Equations

### A.1.3.1. Objective function

The objective function, shown in Equation (A.1), is the sum of all costs over the chosen period, including the annualized investment costs as well as the fixed and variable O&M costs. For some storage options, another CAPEX-related cost proportional to the energy capacity in €/kWh is accounted for ( $annuity_{str}^{en}$ ).

$$COST = (\sum_{tec} [(Q_{tec} - q_{tec}^{ex}) \times annuity_{tec}] + \sum_{str} (VOLUME_{str} \times annuity_{str}^{en}) + \sum_{tec} (Q_{tec} \times fO\&M_{tec}) + \sum_{tec} \sum_h (G_{tec,h} \times (vO\&M_{tec} + e_{tec} SCC_{CO_2}))) / 1000 \quad (A.1)$$

Where  $Q_{tec}$  represents the production capacities,  $q_{tec}^{ex}$  represents the existing capacity (notably for hydro-electricity technologies with long lifetime),  $VOLUME_{str}$  is the energy storage capacity in GWh,  $S_{str}$  is the power capacity of the storage option in GW,  $annuity$  is the annualized investment cost,  $fO\&M$  and  $vO\&M$  respectively represents fixed and variable operation and maintenance costs,  $G_{tec,h}$  is the hourly generation of each technology,  $e_{tec}$  is the specific emission of each technology in tCO<sub>2</sub>/GWh of power production and  $SCC_{CO_2}$  is the social cost of carbon in €/tCO<sub>2</sub>.

### A.1.3.2. Adequacy equations

Energy demand must be met for each hour. If energy production exceeds energy demand, the excess energy can be either sent to storage units or curtailed (Equations A.2, A.3, A.4, A.5a-d and A.6).

$$\sum_{elec} G_{elec,h} \geq demand_{elec,h} + \sum_{str_{elec}} STORAGE_{str_{elec},h} + \sum_{conv_{elec}} CONVERT_{conv_{elec},h} + \sum_{ev} CHARGE_{ev,h} \quad (A.2)$$

$$\sum_{gas} G_{gas,h} \geq \sum_{str_{gas}} STORAGE_{str_{gas},h} + \sum_{conv_{gas}} CONVERT_{conv_{gas},h} + \sum_{ice} CHARGE_{ice,h} + demand_{hydrogen,h} \quad (A.3)$$

$$\sum_{heat} G_{heat,h} \geq demand_{heat,h} + \sum_{str_{heat}} STORAGE_{str_{heat},h} \quad (A.4)$$

$$G_{heavy_t,h} \times \eta_{heavy_t}^{vector_t} = demand_{transport,h}^{heavy_t} \quad (A.5a)$$

$$G_{light_t,h} \times \eta_{light_t}^{vector_t} = demand_{transport,h}^{light_t} \quad (A.5b)$$

$$G_{bus,h} \times \eta_{bus_t}^{vector_t} = demand_{transport,h}^{bus_t} \quad (A.5c)$$

$$G_{train_t,h} \times \eta_{train_t}^{ev_t} = demand_{transport,h}^{train_t} \quad (A.5d)$$

$$G_{electrolysis,h} \geq demand_{hydrogen,h} \quad (A.6)$$

Where  $G_{elec,h}$ ,  $G_{gas,h}$ ,  $G_{heat,h}$  is the energy produced by electricity, gas and heat technologies at hour  $h$  and  $STORAGE_{str_{elec},h}$ ,  $STORAGE_{str_{gas},h}$ ,  $STORAGE_{str_{heat},h}$  is the energy entering storage electricity, gas and heat storage technologies at hour  $h$ .  $CONVERT_{conv_{elec},h}$  is the energy conversion from electricity to other energy carriers and  $CONVERT_{conv_{gas},h}$  is the energy conversion from gas to other carriers at hour  $h$  and  $CHARGE_{ice,h}$  is the charging of internal combustion engine vehicles and  $CHARGE_{ev,h}$  is the charging of electric vehicles at hour  $h$ . For each transport category the energy demand in vehicle.km should be satisfied either by *ev* or *ice* as transport energy carrier options ( $vector_t$ ), and the conversion from the energy in gas or electricity form to the demand by transport category ( $demand_{transport,h}^{heavy_t}$ ,  $demand_{transport,h}^{light_t}$  and  $demand_{transport,h}^{bus_t}$ ) in vehicle.km is done by the vehicle efficiency, which depends on both the energy carrier and the transport category;  $\eta_{cat_t}^{vector_t}$ . We only consider the electricity to satisfy the trains' demand.

According to Vogl et al. (2018), the coal demand for steel industry can be replaced by hydrogen. Therefore, we define an hourly hydrogen demand for steel industry ( $demand_{hydrogen,h}$ ) which should be satisfied (Equation A.6) beside other adequacy equations.

### A.1.3.3. Variable renewable power production

For each variable renewable energy (VRE) technology, for each hour, the hourly power production is given by the hourly capacity factor profile multiplied by the installed capacity available (Equation A.7).

$$G_{vre,h} = Q_{vre} \times cf_{vre,h} \quad (A.7)$$

Where  $G_{vre,h}$  is the energy produced by each VRE resource at hour  $h$ ,  $Q_{vre}$  is the installed capacity and  $cf_{vre,h}$  is the hourly capacity factor.

#### A.1.3.4. Energy storage

Energy stored by storage option  $str$  at hour  $h+1$  is equal to the energy stored at hour  $h$  plus the difference between the energy entering and leaving the storage option at hour  $h$ , accounting for charging and discharging efficiencies (Equation A.8):

$$SOC_{str,h+1} = SOC_{str,h} + (STORAGE_{str,h} \times \eta_{str}^{in}) - \left(\frac{G_{str,h}}{\eta_{str}^{out}}\right) \quad (A.8)$$

Where  $SOC_{str,h}$  is the state of charge of the storage option  $str$  at hour  $h$ , while  $\eta_{str}^{in} \in [0,1]$  and  $\eta_{str}^{out} \in [0,1]$  are the charging and discharging efficiencies.

#### A.1.3.5. Secondary reserve requirements

Three types of operating reserves are defined by ENTSO-E (2013), depending on their activation speed. The fastest reserves are Frequency Containment Reserves (FCRs), which must be able to be on-line within 30 seconds. The second group is made up of Frequency Restoration Reserves (FRRs), in turn divided into two categories: a fast, automatic component (aFRRs), also called ‘secondary reserves’, with an activation time of no more than 7.5 min; and a slow manual component (mFRRs), or ‘tertiary reserves’, with an activation time of no more than 15 min. Finally, reserves with a startup-time beyond 15 minutes are classified as Replacement Reserves (RRs).

Each category meets specific system needs. The fast FCRs are useful in the event of a sudden break, like a line fall, to avoid system collapse. FRRs are useful for variations over several minutes, such as a decrease in wind or PV output. Finally, the slow RRs act as a back-up, slowly replacing FCRs or FRRs when the system imbalance lasts more than 15 minutes.

In the model we only consider FRRs, since they are the most heavily impacted by the inclusion of VRE. FRRs can be defined either upwards or downwards, but since the electricity output of VREs can be curtailed, we consider only upward reserves.

The quantity of FRRs required to meet ENTSO-E’s guidelines is given by Equation (A.9). These FRR requirements vary with the variation observed in the production of renewable energies. They also depend on the observed variability in demand and on forecast errors:

$$\sum_{frr} RSV_{frr,h} = \sum_{vre} (\varepsilon_{vre} \times Q_{vre}) + demand_h \times (1 + \delta_{variation}^{load}) \times \delta_{uncertainty}^{load} \quad (A.9)$$

Where  $RSV_{frr,h}$  is the required hourly reserve capacity from each of the reserve-providing technologies (dispatchable technologies) indicated by the subscript  $frr$ ;  $\varepsilon_{vre}$  is the additional FRR requirement for VRE because of forecast errors,  $\delta_{variation}^{load}$  is the load variation factor and  $\delta_{uncertainty}^{load}$  is the uncertainty factor in the load because of hourly demand forecast errors. The method for calculating these various coefficients according to ENSTO-E guidelines is detailed by Van Stiphout et al. (2017).

#### A.1.3.6. Energy-generation-related constraints

The relationship between hourly-generated energy and installed capacity can be calculated using Equation (A.10). Since the chosen time slice for the optimization is one hour, the capacity enters the equation directly instead of being multiplied by the time slice value.

$$G_{tec,h} \leq Q_{tec} \quad (A.10)$$

The installed capacity of all the dispatchable technologies should be more than the electricity generation required of those technologies to meet demand; it should also satisfy the secondary reserve requirements. Installed capacity for dispatchable technologies can therefore be expressed by Equation (A.11).

$$Q_{frr} \geq G_{frr,h} + RSV_{frr,h} \quad (A.11)$$

Monthly available energy for the hydroelectricity generated by lakes and reservoirs is defined using monthly lake inflows (Equation A.12). This means that energy stored can be used within the month but not across months. This is a parsimonious way of representing the non-energy operating constraints faced by dam operators, as in Perrier (2018).

$$lake_m \geq \sum_{h \in m} G_{lake,h} \quad (A.12)$$

Where  $G_{lake,h}$  is the hourly power production by lakes and reservoirs, and  $lake_m$  is the maximum electricity that can be produced from this energy resource in one month.

#### A.1.3.7. Energy conversion

Energy generated by any energy conversion technology should include the conversion efficiency of the conversion technology. Equation (A.13) relates the energy generation and generation by each conversion technology.

$$G_{conv,h} = \eta^{conv} \times CONVERT_{conv,h} \quad (A.13)$$

Where  $\eta^{conv}$  is the conversion efficiency of the energy conversion technology  $conv$ , and  $CONVERT_{conv,h}$  is the converted energy by the same conversion technology at hour  $h$ .

#### A.1.3.8. Charging of transport technologies

Electric vehicles and internal combustion engine vehicles have different charging profiles. Equation (A.14) applies these charging profiles;

$$CHARGE_{transport,h} = profile_h^{transport} \times Q_{transport} \quad (A.14)$$

Where  $CHARGE_{transport,h}$  is the hourly charging of each transport technology (both EVs and ICEs for all four transport categories),  $profile_h^{transport}$  is the predefined hourly charging profile of each of the transport technologies and  $Q_{transport}$  is the charging capacity of transport technology  $transport$ .

We consider an average of one charge per week for each transport technology, and since the energy can be stored in the vehicle during the whole one week, the transport demand that should be satisfied is considered to have a weekly adequacy. The hourly demand of transport in vehicle.km should be satisfied from Equations (A.5a-d) and the charging profiles should be applied to account for the charging behavior of different transport technologies from Equation (A.14). We define



Equation (A.15) to keep both charging and demand constraints above and to let the vehicles choose the day of charging during the week;

$$\sum_{h \in w} CHARGE_{transport,h} = \sum_{h \in w} G_{transport,h} \quad (A.15)$$

The storage volume of each transport technology accounts for an upper limit for the weekly charge and weekly energy consumption of it. While this storage volume is free of charge for ICE vehicles, electric vehicles' main cost component is this battery storage volume. Therefore, we define the reservoir size (storage volume) for each transport technology (Equation A.16).

$$\sum_{h \in w} CHARGE_{transport,h} \leq RESERVOIR_{transport} \quad (A.16)$$

Where  $RESERVOIR_{transport}$  accounts for the reservoir size of each transport technology (kWh<sub>e</sub> for electric vehicles and kWh<sub>th</sub> for ICE vehicles).

#### **A.1.3.9. Inclusion of heat networks**

Heat can be produced by two different technology classes: distributed technologies such as resistive heating technology, and centralized technologies such as central boilers. Decentralized heating technologies use electricity or gas from the network and provide heating for the local demand, therefore no heat network is needed. On the other hand, the centralized technologies produce heat in large quantities and distribute it for the demand in different locations, which require a heat network. Equation (A.17) separates the central heating technologies and define a heat network capacity for the distribution of produced heat;

$$Q_{heat-net} \geq Q_{central} \quad (A.17)$$

Where  $Q_{heat-net}$  is the heat network capacity and  $Q_{central}$  is the installed capacity of each central heat production technology in kW<sub>th</sub>.

Equation (17) allows the heat network to have lower capacity than all the central heating technologies combined, depending on the optimal dispatching of each of them. Another equation is needed to restrict the central heating technologies to pass through the heat network (Equation 18);

$$G_{heat-net,h} = \sum_{central} G_{central,h} \quad (A.18)$$

Where  $G_{heat-net,h}$  is the heat generation passed through heat network and  $G_{central,h}$  is the heat generation by each central heating technology at hour  $h$ .

#### **A.1.3.10. Operational constraints of conversion technologies**

For open-cycle and combined-cycle gas turbines, there are some safety- and maintenance-related breaks. Equations (A.19), (A.20) and (A.21) limit the annual power production for each of these plants to their maximum annual capacity factors:

$$\sum_h G_{ocgt,h} \leq Q_{ocgt} \times cf_{ocgt} \times 8760 \quad (A.19)$$

$$\sum_h G_{ccgt,h} \leq Q_{ccgt} \times cf_{ccgt} \times 8760 \quad (A.20)$$

$$\sum_h G_{ccgt-ccs,h} \leq Q_{ccgt-ccs} \times cf_{ccgt-ccs} \times 8760 \quad (A.21)$$

Where  $cf_{ocgt}$  and  $cf_{ccgt}$  are the capacity factors of OCGT and CCGT power plants.

The hydrogen produced from electrolysis (power-to-gas conversion) is either consumed directly in the industry (therefore we make the assumption of local electrolysis for industrials) or injected to the gas network. Because of different thermochemical properties of hydrogen, it cannot be injected at any rate to the gas network. Equations (A.22), (A.23) and (A.24) limit the hydrogen in that can exist in the gas network as a proportion of the overall existing gas in this network both in the storage level and in the distribution/transmission level;

$$G_{electrolysis,h} \leq \tau^{hydrogen} \times SOC_{gastank,h} + demand_{hydrogen,h} \quad (A.22)$$

$$G_{electrolysis,h} \leq \tau^{hydrogen} \times \sum_{gas} G_{gas,h} + demand_{hydrogen,h} \quad (A.23)$$

$$\sum_h G_{electrolysis,h} \leq \tau^{hydrogen} \times \sum_{gas \neq gastank,h} G_{gas,h} + \sum_h demand_{hydrogen,h} \quad (A.24)$$

Where  $G_{electrolysis,h}$  is the energy value of hydrogen injected to gas network from electrolysis at hour  $h$ ,  $\tau^{hydrogen}$  is the maximal relative energy share of hydrogen to the overall gas in the gas network which can be different for different countries depending on the capability of gas network in hosting hydrogen.  $SOC_{gastank,h}$  is the state of charge of gas storage, which is the energy value of overall existing gas in the gas network and  $\sum_{gas} G_{gas,h}$  is the overall gas production at hour  $h$ . Equation (A.22) limits the relative share of hydrogen to other gas options in the storage infrastructures and Equation (A.23) limits the relative share of hydrogen in the gas network. Equation (A.24) makes sure that the overall hydrogen that is produced is not more than the capacity of the gas network.

#### **A.1.3.11. Nuclear-power-related constraints**

Addition of nuclear power plants to the model brings three main constraint type equations: ramping up and ramping down rates (because we allow these plants to be used in load-following mode, Loisel et al., 2018) and the annual maximal capacity factor.

Nuclear power plants have limited flexibility, so definitions of hourly ramp-up and ramp-down rates are essential to model them accurately. Equations (A.25) and (A.26) limit the power production of nuclear power plants with these ramping constraints:

$$G_{nuc,h+1} + RSV_{nuc,h+1} \leq G_{nuc,h} + r_{nuc}^{up} \times Q_{nuc} \quad (A.25)$$

$$G_{nuc,h+1} \geq G_{nuc,h}(1 - r_{nuc}^{down}) \quad (A.26)$$

Where  $G_{nuc,h+1}$  is the nuclear power production at hour  $h + 1$ ,  $G_{nuc,h}$  is the nuclear power production at hour  $h$ ,  $RSV_{nuc,h+1}$  is the reserve capacity provided by nuclear power plants at hour  $h + 1$  and  $r_{nuc}^{up}$  and  $r_{nuc}^{down}$  are the ramp-up and ramp-down rates for nuclear power production.

The nuclear power plants' capacity factor should also be limited by safety and maintenance constraints. Equation (A.27) quantifies this limitation:

$$\sum_h G_{nuc,h} \leq Q_{nuc} \times cf_{nuc} \times 8760 \quad (A.27)$$

Where  $cf_{nuc}$  is the maximum annual capacity factor of nuclear power plants.

### A.1.3.12. Storage-related constraints

To prevent optimization leading to a very high quantity of stored energy in the first hour represented and a low quantity in the last hour, we add a constraint to ensure the replacement of the consumed stored energy in every storage option (Equation A.28):

$$SOC_{str,0} = SOC_{str,8759} + (STORAGE_{str,8759} \times \eta_{str}^{in}) - \left(\frac{G_{str,8759}}{\eta_{str}^{out}}\right) \quad (A.28)$$

While Equations (A.8) and (A.26) define the storage mechanism and constraint in terms of power, we also limit the available volume of energy that can be stored by each storage option (Equation A.29):

$$SOC_{str,h} \leq VOLUME_{str} \quad (A.29)$$

Equation (A.30) limits the entry of energy into the storage units to the charging capacity of each storage unit. Similarly, we consider a charging capacity lower than or equal to the discharging capacity (mainly to limit the charging capacity of batteries) which means that the charging capacity cannot exceed the discharging capacity.

$$SOC_{str,h} \leq S_{str} \leq Q_{str} \quad (A.30)$$

### A.1.3.13. Resource availability related constraints

The maximum installed capacity of each technology depends on land-use-related constraints, social acceptance, the maximum available natural resources and other technical constraints; therefore, a technological constraint on maximum installed capacity is defined in Equation (A.31) where  $q_{tec}^{max}$  is this capacity limit:

$$Q_{tec} \leq q_{tec}^{max} \quad (A.31)$$

Renewable gas production technologies are limited due to land-use and agricultural constraints. Equation (A.32) limits the annual renewable gas production from each of two renewable gas production technologies; methanization and pyro-gasification of biomass.

$$\sum_{h=0}^{8759} G_{biogas,h} \leq g_{biogas}^{max} \quad (A.32)$$

Where  $G_{biogas,h}$  is the hourly biogas production from each of renewable gas production technologies and  $g_{biogas}^{max}$  is the maximal yearly biogas that can be produced from each of renewable gas production technologies, both in energy values.

Methanation consists of the Sabatier reaction of hydrogen produced from electrolysis of water and green CO<sub>2</sub> produced as a by-product of methanization process. Implication of this limit in the overall methane production from methanation process is presented in Equation (A.33):

$$\sum_{h=0}^{8759} CONVERT_{methanation,h} \leq \sum_{h=0}^{8759} G_{methanization,h} \times \gamma_{methanization}^{CO_2} \quad (A.33)$$

Where  $CONVERT_{methanation,h}$  accounts for the hourly methane produced from power-to-methane (methanation) process,  $G_{methanization,h}$  is the hourly biogas production from methanization process and  $\gamma_{methanization}^{CO_2}$  is the relative share of carbon dioxide to biogas produced from methanization process.

The captured carbon dioxide can't be stored infinitely, and geographical and social constraints limit the exploitation of CCS technology. Equation (A.34) limits the captured CO<sub>2</sub> to the available offshore and onshore storage formations;

$$\varphi_{CO_2}^{max} \geq \sum_h G_{ccgt-ccs,h} \times \tau_{ccgt-ccs} \times e_{ccgt} \quad (A.34)$$

Where  $\varphi_{CO_2}^{max}$  is the maximal CO<sub>2</sub> storage potential,  $G_{ccgt-ccs,h}$  is hourly power production from CCGT power plants equipped with CCS units,  $\tau_{ccgt-ccs}$  is the carbon capture rate of post combustion CCS units, and  $e_{ccgt}$  is the specific emission of CCGT power plant with natural gas (considered with no CCS input).

## Appendix 2. Installed capacities and annual energy production for simulation with coarse temporal resolutions

In order to better visualize the accuracy of each variant case, the energy mix and the associated errors must be studied. Tables A.4 and A.5 show the installed capacity and the annual energy production for the base case with hourly temporal resolution and for each variant case with coarser temporal resolution and the error associated with it.

Table A.4. Installed capacities of energy production, conversion and storage technologies for different temporal resolutions and their error from the base case of hourly resolution

Technology Installed Capacity (GW)	Temporal Resolution						
	1-h	2-h	error	4-h	error	8-h	error
<i>Energy Production</i>							
<i>Offshore wind</i>	0.0	0.0	0.00%	0.0	0.00%	0.0	0.00%
<i>Onshore Wind</i>	80.21	80.53	0.40%	80.35	0.17%	81.62	1.76%
<i>Solar PV</i>	79.35	81.84	3.14%	85.59	7.86%	86.96	9.59%
<i>Hydroelectricity</i>	20.4	20.4	0.00%	20.4	0.00%	20.4	0.00%
<i>Nuclear energy</i>	22.6	22.26	1.50%	21.77	3.67%	21.21	6.15%
<i>Fossil Gas</i>	0.0	0.0	0.00%	0.0	0.00%	0.0	0.00%
<i>Methanization</i>	17.35	17.35	0.00%	17.35	0.00%	17.35	0.00%
<i>Pyro-gasification of Biomass</i>	0.0	0.0	0.00%	0.0	0.00%	0.0	0.00%
<i>Energy Conversion</i>							
<i>OCGT</i>	2.14	2.15	0.47%	1.88	12.15%	2.2	2.80%
<i>CCGT</i>	5.03	5.22	3.78%	5.88	16.90%	6.36	26.44%
<i>CCGT-CCS</i>	5.72	5.52	3.50%	5.35	6.47%	4.99	12.76%
<i>Electrolysis</i>	6.37	6.35	0.31%	6.37	0.00%	6.37	0.00%
<i>Methanation</i>	3.48	3.48	0.00%	3.47	0.29%	3.46	0.57%
<i>Central heat pump</i>	26.42	26.67	0.95%	27.45	3.90%	27.82	5.30%
<i>Individual heat pump</i>	41.84	41.60	0.57%	41.23	1.46%	40.92	2.20%
<i>Resistive heating</i>	17.78	17.96	1.01%	17.50	1.57%	17.92	0.79%
<i>Central gas boiler</i>	0.0	0.0	0.00%	0.0	0.00%	0.0	0.00%
<i>Individual gas boiler</i>	0.0	0.0	0.00%	0.0	0.00%	0.0	0.00%
<i>Energy Storage</i>							
<i>Battery storage</i>	4.72	5.11	8.26%	5.19	9.96%	5.46	15.68%
<i>Battery storage (GWh)</i>	0.0	0.0	0.00%	0.0	0.00%	0.0	0.00%
<i>Gas Storage</i>	24.61	24.55	0.24%	24.66	0.20%	25.48	3.54%
<i>Gas Storage (TWh)</i>	134.6	134.6	0.00%	134.6	0.00%	134.6	0.00%
<i>Individual thermal energy storage</i>	35.8	18.15	49.30%	9.23	74.22%	3.57	90.03%
<i>Individual thermal energy storage (GWh)</i>	44.31	36.30	18.08%	36.93	16.66%	28.558	35.55%
<i>Central thermal energy storage</i>	46.25	46.76	1.10%	46.99	1.60%	47.689	3.11%
<i>Central thermal energy storage (TWh)</i>	31.58	31.28	0.95%	30.26	4.17%	29.644	6.12%
<i>Heat Network</i>	46.25	46.76	1.10%	46.99	1.60%	47.69	3.11%

Table A.5. Annual energy production from energy production, conversion and storage technologies for different temporal resolutions and their error from the base case of hourly resolution

Technology Energy Supply (TWh/year)	Temporal Resolution						
	1-h	2-h	error	4-h	error	8-h	error
<i>Energy Production</i>							
<i>Offshore wind</i>	0.0	0.0	0.00%	0.0	0.00%	0.0	0.00%
<i>Onshore Wind</i>	228.16	229.07	0.40%	228.55	0.17%	232.15	1.75%
<i>Solar PV</i>	112.83	116.38	3.15%	121.71	7.87%	123.66	9.60%
<i>Hydroelectricity</i>	43.8	43.8	0.00%	43.8	0.00%	43.8	0.00%
<i>Nuclear energy</i>	166.99	162.59	2.63%	157.94	5.42%	153.02	8.37%
<i>Fossil Gas</i>	0.0	0.0	0.00%	0.0	0.00%	0.0	0.00%
<i>Methanization</i>	152.0	152.0	0.00%	152.0	0.00%	152.0	0.00%
<i>Pyro-gasification of Biomass</i>	0.0	0.0	0.00%	0.0	0.00%	0.0	0.00%
<i>Energy Conversion</i>							
<i>OCGT</i>	1.04	1.05	0.96%	0.86	17.31%	1	3.85%
<i>CCGT</i>	4.54	4.78	5.29%	5.33	17.40%	5.81	27.97%
<i>CCGT-CCS</i>	8.59	8.33	3.03%	8.10	5.70%	7.51	12.57%
<i>Electrolysis</i>	51.21	51.18	0.06%	51.17	0.08%	51.18	0.06%
<i>Methanation</i>	16.57	16.51	0.36%	16.58	0.06%	16.5	0.42%
<i>Central heat pump</i>	117.13	117.34	0.18%	118.38	1.07%	118.47	1.14%
<i>Individual heat pump</i>	329.49	328.76	0.22%	326.90	0.79%	325.59	1.18%
<i>Resistive heating</i>	19.18	19.48	1.56%	19.89	3.70%	20.86	8.76%
<i>Central gas boiler</i>	0.0	0.0	0.00%	0.0	0.00%	0.0	0.00%
<i>Individual gas boiler</i>	0.0	0.0	0.00%	0.0	0.00%	0.0	0.00%
<i>Energy Storage</i>							
<i>Battery storage</i>	0.0	0.0	0.00%	0.0	0.00%	0.0	0.00%
<i>Gas Storage</i>	25.61	25.53	0.31%	25.59	0.08%	25.55	0.23%
<i>Individual thermal energy storage</i>	7.93	6.56	17.28%	5.90	25.60%	4.02	49.31%
<i>Central thermal energy storage</i>	34.06	33.85	0.62%	32.81	3.67%	32.72	3.93%
<i>Heat Network</i>	151.19	151.19	0.00%	151.19	0.00%	151.19	0.00%
<i>EV train</i>	30	30	0.00%	30	0.00%	30	0.00%
<i>EV light</i>	3.98	3.97	0.25%	3.96	0.50%	3.97	0.25%
<i>EV heavy</i>	0.0	0.0	0.00%	0.0	0.00%	0.0	0.00%
<i>EV bus</i>	0.0	0.0	0.00%	0.0	0.00%	0.0	0.00%
<i>ICE light</i>	89.64	89.66	0.02%	89.68	0.04%	89.69	0.06%
<i>ICE heavy</i>	56.97	56.97	0.00%	56.97	0.00%	56.97	0.00%
<i>ICE bus</i>	6.47	6.47	0.00%	6.47	0.00%	6.47	0.00%

### Appendix 3. Installed capacities and annual energy production for representative period selection methods

Tables A.6 and A.7 show the installed capacity and the annual energy production of each technology for the base case with hourly temporal resolution over the continuous period of a whole year and for each of the representative period precisions.

Table A.6. Installed capacities of energy production, conversion and storage technologies for different periods represented by a week (1 month, two months and three months) and their error from the base case

Technology Installed Capacity (GW)	Represented period by one week						
	base	1M	error	2M	error	3M	error
<i>Energy Production</i>							
<i>Offshore wind</i>	0.0	20	100%	20	100%	20	100%
<i>Onshore Wind</i>	80.21	120	49.61%	120	49.61%	120	49.61%
<i>Solar PV</i>	79.35	70.89	10.66%	43.39	45.31%	40.52	48.94%
<i>Hydroelectricity</i>	20.4	20.4	0%	20.4	0%	20.4	0%
<i>Nuclear energy</i>	22.6	0	100%	0	100%	0	100%
<i>Fossil Gas</i>	0.0	39.6	100%	44.84	100%	20.43	100%
<i>Methanization</i>	17.35	16.01	7.72%	16.86	2.81%	18.03	3.94%
<i>Pyro-gasification of Biomass</i>	0.0	0.0	0%	0.0	0%	0.0	0%
<i>Energy Conversion</i>							
<i>OCGT</i>	2.14	0	100%	0	100%	0	100%
<i>CCGT</i>	5.03	3.92	22.07%	4.094	18.61%	0	100%
<i>CCGT-CCS</i>	5.72	4.19	26.75%	4.97	13.11%	1.336	76.64%
<i>Electrolysis</i>	6.37	6.24	2.04%	6.245	1.96%	6.227	2.24%
<i>Methanation</i>	3.48	4.54	30.46%	2.059	40.83%	0.632	81.84%
<i>Central heat pump</i>	26.42	39.51	49.55%	31.183	18.03%	31.266	18.34%
<i>Individual heat pump</i>	41.84	33.41	20.15%	36.586	12.56%	41.071	1.84%
<i>Resistive heating</i>	17.78	14.77	16.93%	10.738	39.61%	12.36	30.48%
<i>Central gas boiler</i>	0.0	0.0	0%	0.0	0%	0.0	0%
<i>Individual gas boiler</i>	0.0	12.42	100%	13.791	100%	0.0	0%
<i>Energy Storage</i>							
<i>Battery storage</i>	4.72	0.0	100%	0.0	100%	0.0	100%
<i>Battery storage (GWh)</i>	0.0	0.0	0%	0.0	0%	0.0	0%
<i>Gas Storage</i>	24.61	24.88	1.10%	29.31	19.10%	20.045	18.55%
<i>Gas Storage (TWh)</i>	134.6	134.6	0%	134.6	0%	134.6	0%
<i>Individual thermal energy storage</i>	35.8	41.52	15.98%	0.0	100%	0.0	100%
<i>Individual thermal energy storage (GWh)</i>	44.311	82.16	85.42%	0.0	100%	0.0	100%
<i>Central thermal energy storage</i>	46.25	39.86	13.82%	37.47	18.98%	40.88	11.61%
<i>Central thermal energy storage (TWh)</i>	31.58	0.23	99.27%	3.16	90.00%	4.87	84.53%
<i>Heat Network</i>	46.25	39.86	13.82%	37.47	18.98%	40.88	11.61%

Table A.7. Annual energy production from energy production, conversion and storage technologies for different representative week precisions and their error from the base case

Represented period by one week							
<i>Technology Energy Supply (TWh/year)</i>	<b>base</b>	<b>1M</b>	<b>error</b>	<b>2M</b>	<b>error</b>	<b>3M</b>	<b>error</b>
<i>Energy Production</i>							
<i>Offshore wind</i>	0.0	92.07	100%	92.181	100%	92.138	100%
<i>Onshore Wind</i>	228.16	341.31	49.59%	342.097	49.94%	341.79	49.80%
<i>Solar PV</i>	112.83	101.14	10.36%	61.647	45.36%	57.612	48.94%
<i>Hydroelectricity</i>	43.8	43.8	0%	43.8	0%	43.8	0%
<i>Nuclear energy</i>	166.99	0	100%	0	100%	0	100%
<i>Fossil Gas</i>	0.0	35.28	100%	35.293	100%	0.696	100%
<i>Methanization</i>	152.0	126	17.11%	138.602	8.81%	151.994	0%
<i>Pyro-gasification of Biomass</i>	0.0	0.0	0%	0.0	0%	0.0	0%
<i>Energy Conversion</i>							
<i>OCGT</i>	1.04	0.0	100%	0.0	100%	0.0	100%
<i>CCGT</i>	4.54	4.04	11.01%	4.149	8.61%	0.0	100%
<i>CCGT-CCS</i>	8.59	6.34	26.19%	6.513	24.18%	1.919	77.66%
<i>Electrolysis</i>	51.21	50.07	2.23%	50.121	2.13%	49.709	2.93%
<i>Methanation</i>	16.57	20.34	22.75%	10.992	33.66%	3.364	79.70%
<i>Central heat pump</i>	117.13	148.25	26.57%	132.915	13.48%	131.976	12.67%
<i>Individual heat pump</i>	329.49	261.74	20.56%	292.48	11.23%	309.242	6.15%
<i>Resistive heating</i>	19.18	36.27	89.10%	22.261	16.06%	18.62	2.92%
<i>Central gas boiler</i>	0.0	0.0	0%	0.0	0%	0.0	0%
<i>Individual gas boiler</i>	0.0	10.06	100%	12.582	100%	0.0	0%
<i>Energy Storage</i>							
<i>Battery storage</i>	0.0	0	0%	0.0	0%	0.0	0%
<i>Gas Storage</i>	25.61	7.87	69.27%	8.39	67.24%	7.86	69.30%
<i>Individual thermal energy storage</i>	7.93	17.52	120.93%	0.0	100%	0.0	100%
<i>Central thermal energy storage</i>	34.06	2.38	93.01%	17.907	47.43%	18.88	44.57%
<i>Heat Network</i>	151.19	150.63	0.37%	150.82	0.24%	150.86	0.22%
<i>EV train</i>	30	30	0%	30	0%	30	0%
<i>EV light</i>	3.98	0.0	100%	0.0	100%	0.0	100%
<i>EV heavy</i>	0.0	0.0	0%	0.0	0%	0.0	0%
<i>EV bus</i>	0.0	0.0	0%	0.0	0%	0.0	0%
<i>ICE light</i>	89.64	97.92	9.24%	97.92	9.24%	97.92	9.24%
<i>ICE heavy</i>	56.97	56.97	0%	56.97	0%	56.97	0%
<i>ICE bus</i>	6.47	6.47	0%	6.47	0%	6.47	0%



## Appendix 4. Installed capacities and annual energy supply for each temporal resolution for the case with no nuclear power

Tables A.8 and A.9 show the installed capacity and the annual energy production for the base case with hourly temporal resolution and for each variant case with coarser temporal resolution and the error associated with it, for the variant case where there is no nuclear power.

Table A.8. Installed capacities of energy production, conversion and storage technologies for different temporal resolutions and their error from the base case of hourly resolution for the case with no nuclear power

Technology Installed Capacity (GW)	Temporal Resolution						
	1-h	2-h	Error	4-h	Error	8-h	Error
<i>Energy Production</i>							
<i>Offshore wind</i>	6.04	5.71	5.46%	5.43	10.10%	5.69	5.79%
<i>Onshore Wind</i>	120	120	0.00%	120	0.00%	120	0.00%
<i>Solar PV</i>	122.46	125.8	-2.73%	85.59	30.11%	128.25	4.73%
<i>Hydroelectricity</i>	20.4	20.4	0.00%	20.4	0.00%	20.4	0.00%
<i>Nuclear energy</i>	0	0	0.00%	0	0.00%	0	0.00%
<i>Fossil Gas</i>	53.51	53.11	0.75%	48.88	8.65%	50.44	5.74%
<i>Methanization</i>	17.35	17.35	0.00%	17.35	0.00%	17.35	0.00%
<i>Pyro-gasification of Biomass</i>	0.0	0.0	0.00%	0.0	0.00%	0.0	0.00%
<i>Energy Conversion</i>							
<i>OCGT</i>	10.43	10.28	1.44%	8.47	18.79%	9.42	9.68%
<i>CCGT</i>	7.96	8.19	2.89%	8.29	4.15%	7.75	2.64%
<i>CCGT-CCS</i>	8.82	8.59	2.61%	8.39	4.88%	8.55	3.06%
<i>Electrolysis</i>	8.09	8.03	0.74%	7.97	1.48%	7.94	1.85%
<i>Methanation</i>	3.66	4.16	13.66%	4.26	16.39%	4.36	19.13%
<i>Central heat pump</i>	21.52	22.48	4.46%	23.89	11.01%	24.05	11.76%
<i>Individual heat pump</i>	44.3	43.52	1.76%	42.08	5.01%	41.82	5.60%
<i>Resistive heating</i>	30.3	30.22	0.26%	30.91	2.01%	31.22	3.04%
<i>Central gas boiler</i>	0.0	0.0	0.00%	0.0	0.00%	0.0	0.00%
<i>Individual gas boiler</i>	0.0	0.0	0.00%	0.0	0.00%	0.0	0.00%
<i>Energy Storage</i>							
<i>Battery storage</i>	12.4	12.32	0.65%	11.69	5.73%	11.16	10.00%
<i>Gas Storage</i>	53.51	53.11	0.75%	48.88	8.65%	38.76	27.56%
<i>Gas Storage (TWh)</i>	134.6	134.6	0.00%	134.6	0.00%	134.6	0.00%
<i>Individual thermal energy storage</i>	52.83	34.92	33.90%	26.67	49.52%	9.44	82.13%
<i>Central thermal energy storage</i>	43.85	43.32	1.21%	48.45	10.49%	48.65	10.95%
<i>Heat Network</i>	43.85	43.32	1.21%	48.45	10.49%	48.64	10.92%

Although the energy supply and conversion remain nearly identical, storage options can have higher than 10% of error in the required storage power capacity, particularly for the case of individual thermal storage option this error goes up to 80%. However, the impact of temporal resolution variation is marginal in energy system planning and the cost of the energy system.

Table A.9. Annual energy production from energy production, conversion and storage technologies for different temporal resolutions and their error from the base case of hourly resolution for the case with no nuclear power

<b>Temporal Resolution</b>							
<i>Technology Energy Supply (TWh/year)</i>	<b>1-h</b>	<b>2-h</b>	<b>Error</b>	<b>4-h</b>	<b>Error</b>	<b>8-h</b>	<b>Error</b>
<i>Energy Production</i>							
<i>Offshore wind</i>	27.82	26.3	5.46%	24.99	10.17%	26.21	5.79%
<i>Onshore Wind</i>	341.33	341.33	0.00%	341.33	0.00%	341.33	0.00%
<i>Solar PV</i>	174.14	178.89	2.73%	183.23	5.22%	182.37	4.73%
<i>Hydroelectricity</i>	43.8	43.8	0.00%	43.8	0.00%	43.8	0.00%
<i>Nuclear energy</i>	0	0	0.00%	0	0.00%	0	0.00%
<i>Fossil Gas</i>	18.51	16.05	13.29%	14.06	24.04%	13.89	24.96%
<i>Methanization</i>	152.0	152	0.00%	152.0	0.00%	152.0	0.00%
<i>Pyro-gasification of Biomass</i>	0.0	0.0	0.00%	0.0	0.00%	0.0	0.00%
<i>Energy Conversion</i>							
<i>OCGT</i>	2.58	2.53	1.94%	2.33	9.69%	2.52	2.33%
<i>CCGT</i>	6.72	6.94	3.27%	6.94	3.27%	6.52	2.98%
<i>CCGT-CCS</i>	14.4	13.94	3.19%	13.41	6.88%	13.44	6.67%
<i>Electrolysis</i>	53.24	53.2	0.08%	53.11	0.24%	53.1	0.26%
<i>Methanation</i>	14.39	16.23	12.79%	16.87	17.23%	16.91	17.51%
<i>Central heat pump</i>	96.24	99.47	3.36%	103.32	7.36%	102.7	6.71%
<i>Individual heat pump</i>	319.61	315.22	1.37%	307.08	3.92%	306.86	3.99%
<i>Resistive heating</i>	52.74	57.64	9.29%	60.95	15.57%	61.53	16.67%
<i>Central gas boiler</i>	0.0	0.0	0.00%	0	0.00%	0.0	0.00%
<i>Individual gas boiler</i>	0.0	0.0	0.00%	0	0.00%	0.0	0.00%
<i>Energy Storage</i>							
<i>Battery storage</i>	13.71	13.44	1.97%	12.58	8.24%	11.63	15.17%
<i>Gas Storage</i>	83.42	81.72	2.04%	79.34	4.89%	78.28	6.16%
<i>Individual thermal energy storage</i>	10.93	13.66	24.98%	16.38	49.86%	12.17	11.34%
<i>Central thermal energy storage</i>	54.95	51.72	5.88%	47.87	12.88%	48.49	11.76%
<i>Heat Network</i>	151.19	151.19	0.00%	151.19	0.00%	151.19	0.00%
<i>EV train</i>	30	30	0.00%	30	0.00%	30	0.00%
<i>EV light</i>	4	4	0.00%	3.99	0.25%	3.98	0.50%
<i>EV heavy</i>	0.0	0.0	0.00%	0.0	0.00%	0.0	0.00%
<i>EV bus</i>	0.0	0.0	0.00%	0.0	0.00%	0.0	0.00%
<i>ICE light</i>	89.59	89.6	0.01%	89.61	0.02%	89.64	0.06%
<i>ICE heavy</i>	56.97	56.97	0.00%	56.97	0.00%	56.97	0.00%
<i>ICE bus</i>	6.47	6.47	0.00%	6.47	0.00%	6.47	0.00%